Journal of Materials Chemistry A

PERSPECTIVE

View Article Online
View Journal | View Issue

Cite this: J. Mater. Chem. A, 2022, 10, 19572

Balancing charge dissipation and generation: mechanisms and strategies for achieving steady-state charge of contact electrification at interfaces of matter

Chi Kit Ao, Yan Jiang, Linwan Zhang, Chuanyu Yan, Junhao Ma, Changhui Liu, Yuting Jiang, Wanyu Zhang and Siowling Soh *

Static charge generated by contact electrification is a ubiquitous phenomenon. It causes many undesirable consequences in the manufacturing processes of almost all types of industries and our daily lives. On the other hand, the separation of charge by contact electrification has given rise to a diverse variety of novel applications, including harvesting energy for generating electricity and technologies related to sustainability and sensing. However, the phenomena of contact electrification are generally poorly understood. In particular, there is a great need to understand the ways to achieve desired levels of steady-state charge. The steady-state charge achieved by frequent periodic contact electrification is arguably the most important quantity required in continuous operation. This perspective discusses the mechanisms and strategies for obtaining the desired level of steady-state charge at all interfaces of matter, including solid, liquid, and gas. Many studies discussed charge generation, but much less consideration has been placed on another important factor that critically affects the steady-state charge: charge dissipation. We describe the importance of the many fundamental mechanisms of charge dissipation. In addition, we present the factors influencing the mechanisms of charge dissipation (*e.g.*, *via* a toolbox) and the widespread applications of charge dissipation. The importance of charge dissipation thus indicates that the steady-state charge is a balance between charge generation and charge dissipation. We discuss that different rates of charge generation and charge dissipation are useful in different circumstances. Because the dissipation of static charge generated by contact electrification occurs readily into all interfaces of matter, static is, in fact, highly dynamic in nature.

Received 21st April 2022
Accepted 12th August 2022

DOI: 10.1039/d2ta03232e

rsc.li/materials-a

Department of Chemical and Biomolecular Engineering, National University of Singapore, 4 Engineering Drive 4, Singapore 117585, Singapore. E-mail: chessl@nus.edu.sg

Chi Kit Ao received his B.Sc. degree in chemistry from the Chinese University of Hong Kong (CUHK) in 2018. He is currently pursuing his Ph.D. degree at the Department of Chemical and Biomolecular Engineering, National University of Singapore, under the supervision of Prof. Siowling Soh. His research focuses on the fundamentals and applications of electrostatics and surface charge generated by contact electrification. He develops strategies to control the surface charge generated at different interfaces including solid, liquid, and gas.

Siowling Soh received his Ph.D. degree from Northwestern University where he studied under Bartosz Grzybowski. He then worked with George Whitesides at Harvard University as a postdoctoral fellow. His current research in the Department of Chemical and Biomolecular Engineering at the National University of Singapore is highly interdisciplinary. It involves the physical–chemical investigation of the fundamental mechanisms of charge separation at all the interfaces of matter, including solid, liquid, and gas. He studies the materials science of controlling charge separation and develops novel applications. His research interests also include smart materials and the creation of intelligence in materials.

1. Introduction

Contact electrification is the process in which static charge is generated when two surfaces are brought into contact and are then separated. Almost all types of materials can be charged highly by contact electrification, including polymers, inorganic materials, and metals. Contact electrification occurs in all types of contact, including slight touching, rubbing, sliding, rolling, grinding, and fracturing. Hence, contact electrification is a ubiquitous phenomenon. Due to its ubiquity, the static charge generated by contact electrification has a vast range of influences in many circumstances, including activities in our daily lives and in industry.

Contact electrification is useful for a diverse range of applications in many technological fields, such as energy harvesting, sensing, and sustainability (Fig. 1a). A large variety of devices based on contact electrification of surfaces have been reported for harvesting the energy of nature (*e.g.*, wind,[1] rain,[2] rivers,[3] waves,[4] and vibration[5]) and human motion.[6] The harvested energy is then used for powering other devices. Applications of sensing based on contact electrification include environmental sensing (*e.g.*, gas[7] and humidity[8] sensors), health monitoring systems (*e.g.*, monitoring the heart rate and respiration[9]), human–computer interfacing (*e.g.*, force[10] and pressure sensors[11]), and robotics (*e.g.*, motion[12] and sound sensors[13]). Finally, applications related to sustainability include gas filtration,[14] electrostatic separation,[15] pollutant degradation,[16] and antifouling surfaces.[17]

On the other hand, the generation of static charge by contact electrification causes a wide range of undesirable consequences. Problems caused by static charge are encountered in almost all types of industries, including petrochemical, chemical, pharmaceutical, food, textile, automobile, construction, energy, military, biomedical, electronics, and packaging. Static charge causes severe reductions in the efficiency of many manufacturing processes. One important example involves particles (*e.g.*, drug or food powder produced by the pharmaceutical or food industry) that tend to charge highly by contact electrification due to their large surface-area-to-volume ratios. Charged particles often cause large-scale fouling of surfaces (*e.g.*, walls of vessels, pipes, and funnels) due to unwanted aggregation and adhesion of the particles (*i.e.*, as a result of attractive electrostatic forces). Fouling causes the blockage of continuous processes and reduces the ability of vessels to transfer heat.

Another important example involves atmospheric dust. The adhesion of charged dust particles onto surfaces can dramatically reduce the efficiency of many systems, including jamming rotary parts and blocking sunlight from solar panels.[18] The adhesion of charged particles onto surfaces can compromise the quality of products. In the pharmaceutical industry, drug particles charged by contact electrification may aggregate or segregate due to static charge, thus resulting in nonuniform dosages of drug tablets.[19] In addition, charged dust particles contaminate the products (*e.g.*, drugs and food) during the manufacturing process.

Static charge generated by contact electrification routinely causes damage to equipment in industry. Excessive accumulation of static charge on surfaces causes electrostatic discharge (ESD), such as electric sparks, to be produced. Many modern electronic components are highly sensitive to damage caused by ESD—even a simple touch of a finger can often damage advanced types of electronic components (*e.g.*, integrated circuits). The annual cost of ESD damage to the electronics industry is estimated to be in the range of billions of dollars.[20] In addition, ESD can cause explosions when flammable substances are present (*e.g.*, in the petrochemical and chemical industries). An explosion in a research laboratory that caused a post-doctoral researcher to lose one of her arms was possibly due to ESD onto a gas storage tank.[21]

Besides the problems encountered in industry, static charge generated by contact electrification also causes many undesirable effects in many circumstances of our everyday lives. Dust particles charged by contact electrification can adhere onto furniture or screens of computers and phones. A person may experience a mild electric shock due to static charge when touching a conductive surface (*e.g.*, a doorknob or a shopping cart) in dry weather. Electric shocks caused by static charge are unpleasant and may induce anxiety or even trigger panic attacks.

Therefore, there is a need to generate large amounts of static charge by contact electrification for useful applications; on the other hand, there is also a need to eliminate it to mitigate its undesirable consequences. In general, it is important to obtain different amounts of charge for different circumstances. For obtaining the specifically desired amount of charge for a specific circumstance, it is important to understand the fundamental mechanisms of charge generation by contact electrification and strategies for controlling the rate of charge generation. Charge generation is usually the only factor that is important when charge first starts to accumulate on the surfaces by contact electrification. Charge generation has been discussed extensively in numerous reviews.[22–26]

Most circumstances and applications, however, involve the continuous operation of contact electrification for a prolonged period of time (*i.e.*, instead of only the initial build-up of charge). When the charge accumulated on the surfaces approaches the maximum level attainable over a period of continuous contact electrification, the process is certainly not only determined by charge generation—charge dissipation is a critically important factor in determining the level of steady-state charge. In other words, the level of steady-state charge is determined by the balance between charge generation by contact electrification and charge dissipation (Fig. 1b).

Results from our group and other groups have shown the large influence of charge dissipation on steady-state charge at all interfaces of matter *via* many different fundamental mechanisms. One study found that surfaces were able to charge (*i.e.*, to an amount of 1003 $\mu C\ m^{-2}$) many times higher by contact electrification in a high-vacuum environment ($\sim 10^{-6}$ Torr) than under ambient conditions (*i.e.*, due to eliminating the dissipation of charge into normal atmospheric air).[27] This result showed that charge dissipation severely limits the amount of

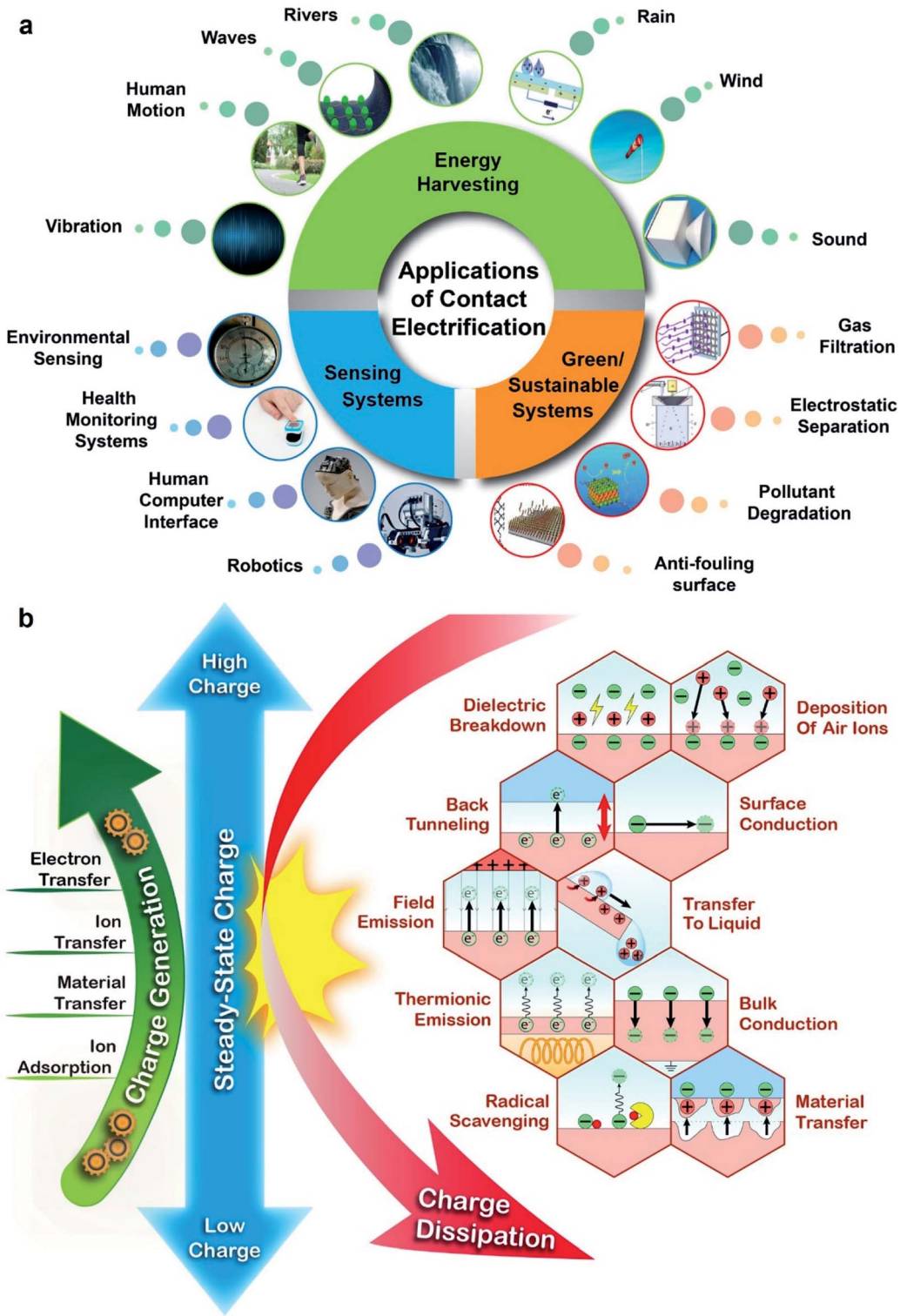

Fig. 1 (a) Important applications of contact electrification in energy harvesting, sustainability, and sensing. Image of rain: reproduced with permission (copyright 2018, Wiley-VCH).[210] Image of wind: credits to Igor Nikushin/Shutterstock. Image of sound: reproduced with permission (copyright 2021, MDPI).[211] Image of gas filtration: reproduced with permission (copyright 2017, American Chemical Society).[212] Image of electrostatic separation: reproduced with permission (copyright 2019, Elsevier).[213] Image of pollutant degradation: reproduced with permission (copyright 2020, Elsevier).[214] Image of an anti-fouling surface: reproduced with permission (copyright 2017, Wiley-VCH).[215] Image of robotics: credits to Jelleke Vanooteghem/Unsplash. Image of a human–computer interface: credits to Possessed Photography/Unsplash. Image of health monitoring systems: credits to Tetiana SHYSHKINA/Unsplash. Image of environmental sensing: credits to Koolshooters/Pexels. Image of vibration: Titima Ongkantong/Shutterstock. Image of human motion: credits to KIRATIYA KUMKAEW/Shutterstock. Image of waves: reproduced with permission (copyright 2017, Elsevier).[216] Image of rivers: Pixabay/Pexels. (b) The steady-state charge from contact electrification is a balance between charge generation and charge dissipation. The fundamental mechanisms of charge generation and charge dissipation are indicated.

charge that can be accumulated onto surfaces by contact electrification. Hence, it is of great importance to consider charge dissipation when determining the level of steady-state charge. However, charge dissipation is a largely overlooked phenomenon in the field of contact electrification. Discussions of dissipation of charge generated by contact electrification have been sparse and scattered among previous studies.

In this perspective, we will first briefly describe the fundamental mechanisms of charge generation by contact electrification. Subsequently, we will provide a detailed discussion of charge dissipation *via* all the interfaces of matter, including gas, liquid, and solid. For each interface, we will discuss the many fundamental mechanisms of charge dissipation. The factors influencing the rates of charge dissipation by the fundamental mechanisms will be discussed and summarized as a toolbox in Table 1. We then illustrate the significance of the fundamental mechanisms by describing the many important applications of charge dissipation. In addition, we will discuss the prevention of charge dissipation for useful applications and circumstances that require charge dissipation for avoiding the undesirable consequences of static charge. These descriptions of charge dissipation are based on results obtained by our research group and other groups around the world. Finally, we will include descriptions of the importance and applications of the different rates of charge generation and charge dissipation that occur simultaneously. In general, this perspective aims to examine the factors for obtaining the required level of steady-state charge for continuous operations in applications, with an emphasis on the importance of charge dissipation.

2. Charge generation

2.1. Mechanisms of charge generation at the solid–solid interface

Static charge is generated when two surfaces of solids are brought into contact and are then separated. This phenomenon has been known since antiquity; the earliest recorded mention was by Plato in ~360 BC.[28] Since then, research has been ongoing continuously and steadily throughout the years. However, the phenomenon is still very poorly understood despite the long history of research. Most of our knowledge about the phenomenon is derived from experimental observations with little fundamental understanding from many different research groups. Most importantly, the fundamental molecular mechanism of generating static charge is poorly understood when the contact involves at least one insulating material. There are three main mechanisms proposed in previous studies: electron transfer, ion transfer, and material transfer (Fig. 2). Without a clear understanding of the fundamental molecular mechanism and the basic conceptual framework, it is thus challenging to develop understanding of the properties and behaviors of the phenomenon in general. It is widely established that electron transfer is the mechanism for the contact electrification between two pieces of metal. Previous studies have found that the work function of the metal is proportional to the amount of charge generated by contact electrification by contacting different types of metals with a reference piece of metal.[29,30] These results convincingly showed that it is the

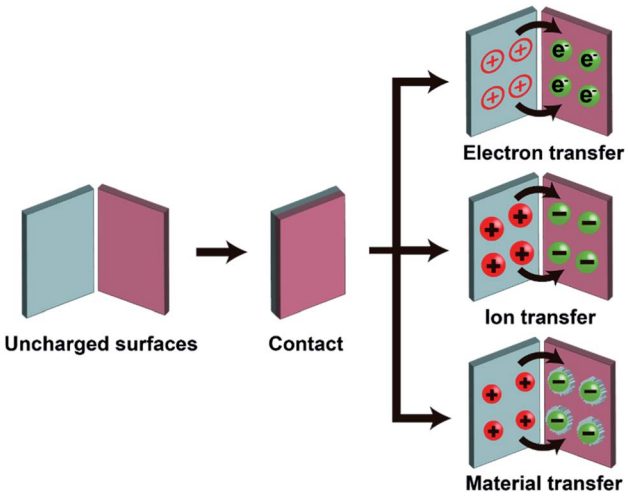

Fig. 2 Charge generation at the solid–solid interface. Scheme illustrates the three fundamental mechanisms (*i.e.*, electron transfer, ion transfer, and material transfer) of contact electrification between two solid surfaces.

transfer of electrons from the metal with a lower work function to the metal with a higher work function that leads to the generation of charge on both surfaces by contact electrification.[30,31] Some previous studies reported that the same mechanism applies to the contact electrification between a metal and an insulating material. These studies found similar correlations between the work function of the metal and the amount of charge generated.[31–35] In recent years, Wang and co-workers have proposed that electron transfer is the dominant mechanism for contact electrification between all types of materials (*i.e.*, including two insulating materials) based on a number of experimental observations (*e.g.*, thermal-induced charge dissipation and analyses of surfaces by Kelvin Force Microscopy, KFM).[36–38]

At the same time, results reported in many previous studies indicated that the fundamental mechanism of contact electrification between two pieces of insulators is due to the transfer of ions from one surface to the other. Whitesides and co-workers have investigated the mechanism of ion transfer between two insulators by contact-charging functionalized polymeric microspheres (*i.e.*, polystyrene microspheres with a diameter of 50–450 μm) with glass beads.[39] The functionalized surfaces of the polymeric microspheres consisted of covalently bonded molecules with ionic functional groups and mobile counterions. After contact electrification, results showed that the polymeric microspheres were charged with the same polarity as the ionic functional groups, whereas the glass beads were charged with the same polarity as the mobile counterions.[39,40] In addition, the number of ionic groups functionalized on the surface was proportional to the amount of charge generated by contact electrification. These results indicated that the mobile counterions transferred from the polymeric microspheres to the glass beads during contact electrification. This transfer of ions from one surface to the other led to charge being generated on both surfaces.

Ion transfer has been proposed to be the mechanism of contact electrification for insulating surfaces (*e.g.*, common types of polymers) in general, even without functionalization of

the surface with any ionic functional groups.[41] The proposed mechanism is based on the adsorption of water molecules from the moisture in the surrounding atmosphere onto surfaces. Water molecules adsorb onto most surfaces readily, including hydrophobic surfaces.[41,42] It has been proposed that specific ions (*i.e.*, H^+ and OH^-) in the adsorbed water transfer preferentially from one surface to the other during contact electrification of two insulating materials for the generation of charge.

A better understanding of this mechanism of ion transfer requires the consideration of how a specific type of ion (*i.e.*, of a specific polarity) preferentially transfers from one surface to another. This preferential transfer of a specific type of ion is necessary for charging one surface positively and another surface negatively. Results from our group showed that the preferential transfer is due to the Lewis basicity/acidity of the polymeric surface.[43] We found that polymers with a higher Lewis basicity are charged positively, whereas polymers with a higher Lewis acidity are charged negatively. The Lewis basicity of a molecule indicates its ability to share electrons; the Lewis acidity of a molecule indicates its ability to accept electrons with another molecule or ion. Hence, a molecule with higher Lewis basicity stabilizes cations, whereas a molecule with higher Lewis acidity stabilizes anions better.

Material transfer is another proposed mechanism of contact electrification (*i.e.*, including contacts between insulating materials) that is related to ion transfer. Instead of molecular ions, it involves the transfer of charged ionic fragments of materials (*e.g.*, nanoscale) from one surface to another. The transfer of fragments of materials was confirmed by both physical (*e.g.*, Atomic Force Microscopy, AFM) and chemical analyses (*e.g.*, X-ray photoelectron spectroscopy, XPS).[44–48] We previously investigated the mechanism of material transfer by performing contact-charging experiments with polydimethylsiloxane (PDMS) of varying softness against polyvinyl chloride (PVC).[49] We found that softer pieces of PDMS generated larger amounts of charge by contact electrification. Analysis by XPS showed that softer pieces of PDMS transferred larger amounts of material to PVC. Therefore, a larger amount of material transfer correlated with a larger amount of charge generated. This direct correlation between material transfer and charge generation suggested that material transfer is the mechanism of contact electrification for insulating materials. We analyzed the phenomenon and proposed the following mechanism of material transfer. First, we found that there was an adhesive force (*e.g.*, van der Waals forces) between the two surfaces when in contact. During separation, this adhesive force caused heterolytic cleavage of chemical bonds on the surfaces of the contacting materials. After cleavage, the charged fragments of materials transferred to the opposite contacting surface, thus giving rise to the generation of charge.

2.2. Mechanisms of charge generation at the solid–liquid interface

Charge separation occurs spontaneously at the solid–liquid interface when the two phases are brought into contact. When a solid surface is immersed in a liquid, the separation of charge causes the surface to charge with a specific polarity and the liquid to have ions of the opposite polarity around the surface (*i.e.*, the electric double layer) (Fig. 3a). Several mechanisms have been proposed for the separation of charge at the solid–liquid interface; the specific type of mechanism may depend on the type of substance involved. For surfaces functionalized with ionic groups, the ionization and dissociation of the groups can lead to the separation of charge at the solid–liquid interface.[50] For example, a surface with carboxylic groups may dissociate when in contact with water according to the reaction $COOH \rightarrow COO^- + H^+$. Another possible mechanism involves the adsorption of ions in the liquid onto the surface as reported in many previous studies. One study reported that the zeta potential of the surface became more negative in basic solution compared to water; on the other hand, the zeta potential of the surface became more positive in acidic solution compared to water.[51] These results suggested that the separation of charge at the solid–liquid interface is due to the adsorption of ions (H^+ and OH^-) from the liquid onto the surface. When a metallic surface is immersed in a liquid, electrons may transfer at the solid–liquid interface. Previous studies showed that a higher work function of the metal caused an insulating oil to charge more positively.[52] More recently, Wang and co-workers proposed that electron transfer and ion transfer occurred simultaneously when a droplet of liquid was placed onto a surface and then removed (*i.e.*, the observed thermal-induced dissipation of charge from the surface).[53–58]

Results from previous studies have shown that the charge can remain on the surface and in the liquid when the two phases are brought into contact and are then separated (*e.g.*, a droplet that slides away from a solid surface).[59–63] Our group previously reported that water droplets that flowed across the surface of solid materials can generate large amounts of electric charge.[59] The experiment involved simply flowing water down a channel or a tube by its own weight (Fig. 3b). We found that a continuous power of ~170 μW was generated at a flow rate of 100 mL min^{-1}. The efficiency of the generated power (*i.e.*, the amount of electric power generated over the gravitational potential energy) was 4% (Fig. 3c).[64–68]

2.3. Mechanism of charge generation at the solid–gas interface

Previous studies have found that when surfaces are exposed to an atmosphere with increasing humidity, they tend to gain charge. For example, silica was found to gain a higher negative electric potential at higher humidity.[69] Similarly, aluminum and chrome plated brass were found to have higher charge densities at higher humidity.[70] This charging effect was proposed to be due to the interaction between the surface and atmospheric water that may contain a reservoir of ions (H^+ and OH^-). The ions of a specific polarity may preferentially adsorb onto the surface of the materials, thus charging the surface. The generation of charge at other types of interfaces is currently being investigated (*e.g.*, the liquid–liquid interface).[22,71–74]

2.4. Triboelectric nanogenerator (TENG)

An important general class of devices that are based on contact electrification are triboelectric nanogenerators (TENGs)

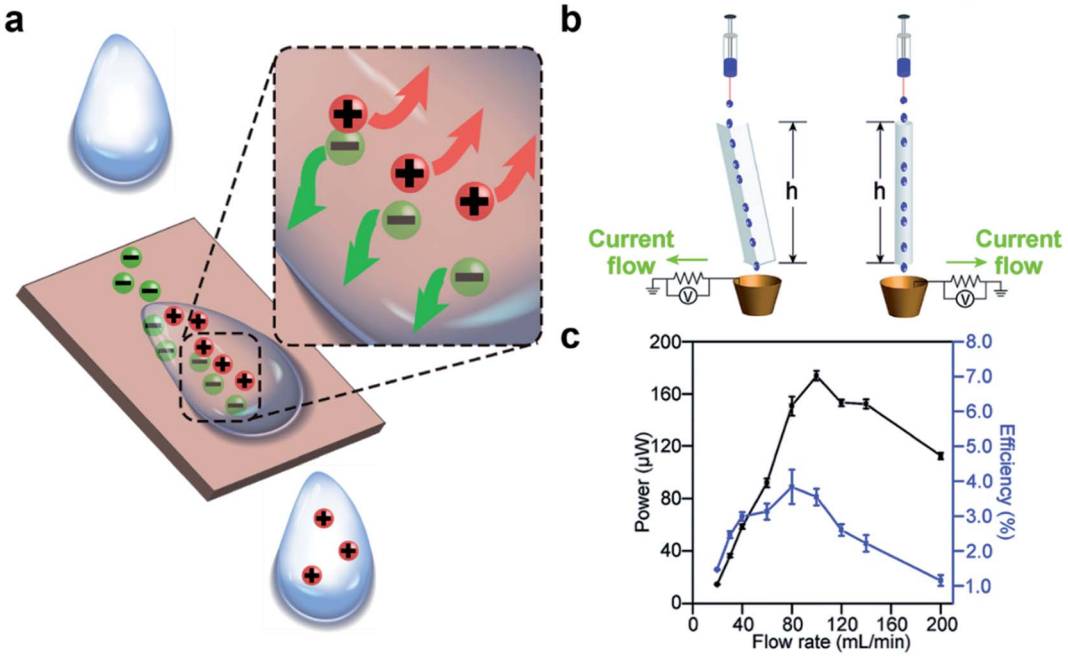

Fig. 3 Charge generation at the solid–liquid interface. (a) Scheme illustrates the mechanism of charge generation at the interface. (b) Water droplets flow down a channel or a tube by their own weight and gain charge by contact electrification. (c) A continuous power of ~170 μW and an energy efficiency (*i.e.*, electric energy produced over loss in the gravitational energy of water) of 4% was generated by a flow rate of water of 100 mL min^{-1}. (b and c) Reproduced with permission (copyright 2015, Royal Society of Chemistry).[59]

developed relatively recently by Wang and co-workers.[75] TENG devices have been developed and shown to be versatile for a diverse range of applications; a few examples include harvesting energy,[76–79] biomedical devices,[80,81] manipulating fluid,[82] generating micro-plasma,[83] and tribotronics.[84] A TENG device essentially converts a certain form of kinetic energy (*e.g.*, motion of humans or natural sources of energy) into an electric current. The main component of a typical TENG device consists of two flat slabs of solids. Each slab of solid is usually composed of two layers: a highly chargeable insulating layer (*e.g.*, polytetrafluoroethylene, PTFE) and a conductive layer (*e.g.*, copper). The two slabs of solids are oriented such that the two insulating layers face each other and the two conductive layers are located on the outside. Both the conductive layers of the two flat slabs of solids are connected electrically to an external circuit *via* wiring for its intended purpose. The energy that the TENG device harvests is often based on a periodic motion, such as vibration (*e.g.*, by people walking frequently across a platform) or continual impact (*e.g.*, periodic flow of water due to waves). This periodic motion causes the two slabs of solids to come into contact and separate in an oscillatory manner. When the two insulating surfaces come into contact, charging of the surfaces occurs by contact electrification; one surface is charged positively while the other surface is charged negatively. Subsequently, charge is induced in the conductive layer because of the charge generated on the insulating surface. In the state at which the two slabs of solids are separated, a substantial amount of charge with a polarity opposite to the polarity of the insulating surface is induced in the conductive layer. In the state at which the two slabs of solids are brought into contact, the proximity of the two oppositely charged insulating surface reduces the amount of charge induced in the conductive layers. Therefore, varying amounts of charge are induced in the conductive layers during the continuous oscillatory and repeated contact and separation of the two slabs of solids. This effect allows an electric current to flow between the conductive layers and the external circuit. This electric current is then used for different applications, such as for providing electric power or charging (*e.g.*, for mass spectrometry and capacitors).

3. Charge dissipation into gas

Besides the generation of charge by contact electrification, charge also dissipates readily into the different interfaces of matter. We will discuss the dissipation of charge into gas, liquid, and solid sequentially.

3.1. Dielectric breakdown

3.1.1. Fundamentals of dielectric breakdown. Dielectric breakdown of gas occurs when the atmospheric gas molecules ionize due to a strong applied electric field. Ionization occurs when the strength of the electric field exceeds the dielectric breakdown strength of the gas, thus causing the gas to become electrically conductive. This process plays a major role in the dissipation of static charge generated by contact electrification on the surfaces of materials. The electric field produced by the static charge may be sufficiently large that it causes dielectric breakdown of the gas and ionization of the gaseous molecules

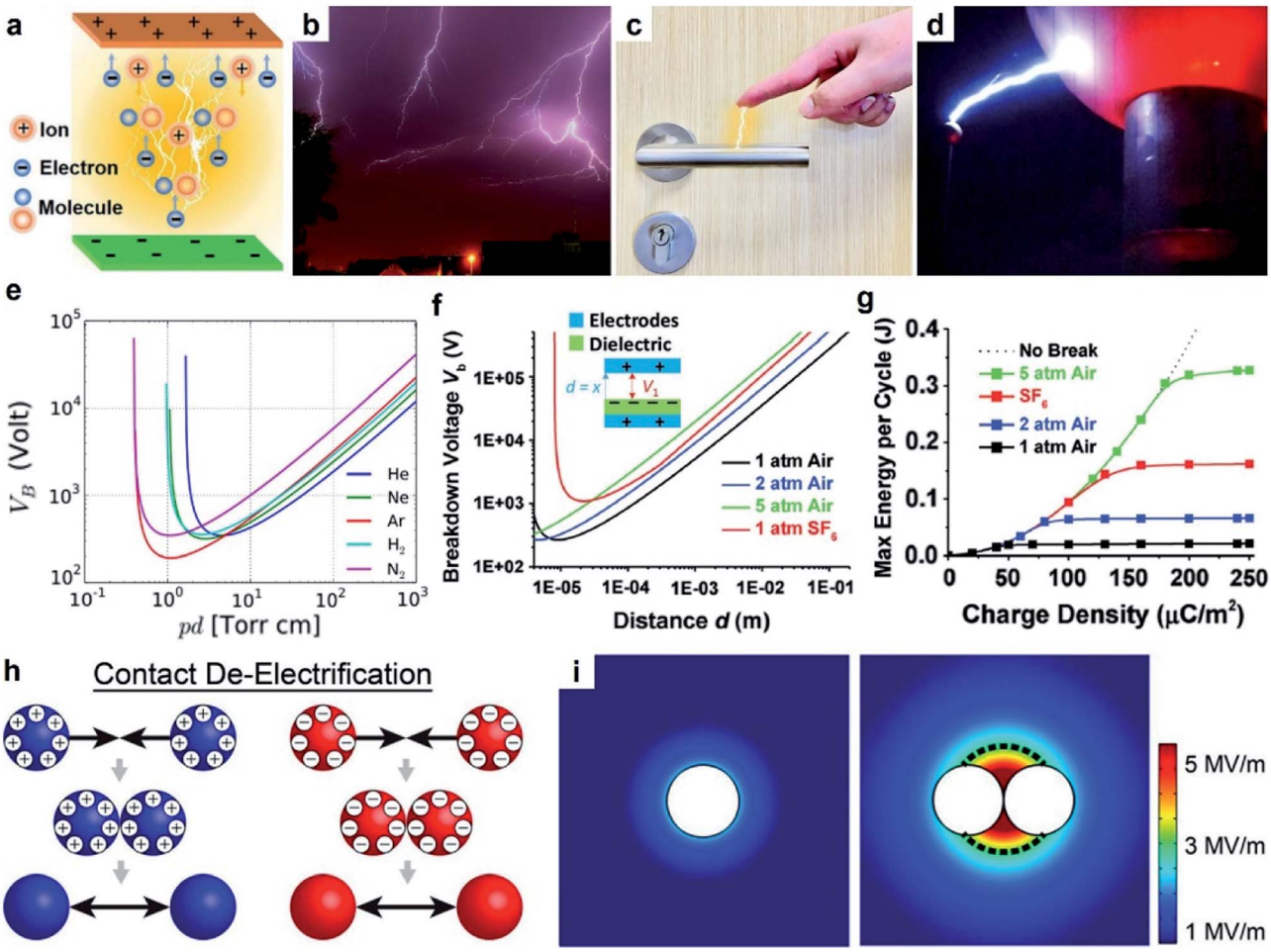

Fig. 4 Charge dissipation into the gaseous atmosphere by dielectric breakdown. (a) Scheme illustrates the mechanism of dielectric breakdown, reproduced with permission (copyright 2020, Wiley-VCH).[85] Images of (b) lightning (credits: Thomas Bresson), (c) electrical shock when a person reaches for a doorknob, and (d) Van de Graaff generator (credits: Z22/Wikimedia Commons). (e) Paschen's curve: breakdown voltage, V_b, against the product of gas pressure, p, and gap distance, d. Curves for different gases are shown, including helium (He), neon (Ne), argon (Ar), hydrogen (H_2) and nitrogen (N_2) (credits: Krishnavedala/Wikimedia Commons). (f) Breakdown voltage, V_b, of air and sulfur hexafluoride (SF_6) at different pressures and gap distances, d. (g) Plot of maximum energy per cycle produced by a TENG device against the charge density for different conditions, reproduced with permission (copyright 2017, Wiley-VCH).[92] (h) Scheme illustrates contact de-electrification. (i) Simulations of the electric field around (left) a single charged particle and (right) two charged particles of the same polarity in contact, reproduced with permission (copyright 2012, American Chemical Society).[93]

(Fig. 4a).[85] The ionization produces positively and negatively charged species in the atmosphere. The charged species of the same polarity with respect to the charged surface are repelled away from the surface, whereas the charged species of the opposite polarity are attracted and deposit onto the surface. The deposition of the oppositely charged species neutralizes the charge on the surface. The charge generated from contact electrification is thus dissipated through this process.

The dielectric breakdown of air due to static charge generated by contact electrification is a widely observed natural phenomenon. A common example is lightning (Fig. 4b). Particles in the atmospheric cloud (*e.g.*, ice crystals) dynamically collide with each other and become charged by contact electrification.[86] The separation and accumulation of charge within the cloud lead to an increasing electric field that eventually exceeds the dielectric breakdown strength of air. Dielectric breakdown of air then occurs between the cloud particles and the ground, or between clouds. The breakdown thus generates an electric current in the form of lightning. Another example is the mild electric shock due to static charge frequently experienced in our lives (Fig. 4c). When a person walks over a carpet, contact electrification between the carpet and the body generates static charge, thus charging up the human body. As the person reaches for a doorknob, the electric field produced by the charge on the hand results in the dielectric breakdown of air between the hand and doorknob (*i.e.*, a phenomenon that lasts ~nanoseconds).[87] The electric current produced by the breakdown then causes the person to experience an electric shock. Another common demonstration of dielectric breakdown of air involves a Van de Graaff generator.[88] A Van de Graaff generator consists of an insulating belt moving over two rollers of different materials. Contact electrification between the belt and

the rollers generates charge on the rollers; one roller becomes positively charged, whereas the other is negatively charged. The rollers then transfer their charges to two separate metal spheres. When the two metal spheres of opposite polarities are brought closer to each other, the strong electric field generated between the spheres causes the dielectric breakdown of air. This phenomenon often produces strong electric sparks between the metal spheres (Fig. 4d). These examples show that dielectric breakdown of air caused by contact electrification is a common occurrence; hence, it is critically important to consider the dielectric breakdown of air when studying contact electrification.

3.1.2. Dielectric breakdown due to a single charged surface. A basic model of charge dissipation from a surface *via* dielectric breakdown involves a single charged material surrounded by a gaseous atmosphere. Two important properties of the material that influence the dissipation of static charge *via* dielectric breakdown are the shape and size. The influence of the shape of a charged surface on its electric field can be determined using the Gauss law. The law states that the flux of the electric field out of an enclosed surface, S, is proportional to the net charge enclosed, as expressed in eqn (1)

$$\oiint_S E \, \mathrm{d}A = \frac{Q}{\varepsilon} \tag{1}$$

where E is the electric field, A is the surface area, Q is the amount of charge, and ε is the permittivity of the gas. For a simple planar surface with uniformly distributed static charge, the electric field from both sides of the surface can be expressed as eqn (2)

$$E = \frac{Q}{2A\varepsilon} \tag{2}$$

where A is the surface area of the planar surface. For a cylindrical surface, the electric field is expressed as eqn (3)

$$E = \frac{Q}{2\pi RL\varepsilon} \tag{3}$$

where R is the radius of the cylinder and L is the length. For a spherical surface, the electric field is expressed as eqn (4)

$$E = \frac{Q}{4\pi R^2\varepsilon} \tag{4}$$

where R is the radius of the sphere.

A common case involves a charged spherical particle in air. Air has a dielectric breakdown strength of $E_{\mathrm{air}} = 3$ MV m^{-1} and a permittivity of $\varepsilon_{\mathrm{air}} = 8.85$ pC V^{-1} m^{-1}. Hence, the maximum charge density of the spherical particle is $\sigma = Q/(4\pi R^2) = E_{\mathrm{air}}\varepsilon_{\mathrm{air}} = 27$ μC m^{-2}. This maximum charge density is on the same order of magnitude as discussed in previous studies for a wide range of particles (*i.e.*, polystyrene beads of 50–450 μm in diameter) coated with ionic groups.[39] These results indicated that the surfaces experience rapid dissipation of static charge *via* dielectric breakdown of air beyond the maximum charge density.

The influence of the size of a charged surface on its electric field can also be determined *via* the Gauss law. Eqn (4) shows that for spherical particles, Q scales with the square of the radius of the particle, R. This scaling relation has been verified by previous investigations.[39,89] The verification by experimental results indicates that the equations and the scaling relation are useful for predicting the dissipation of static charge *via* dielectric breakdown of a single charged material.

3.1.3. Dielectric breakdown between two charged surfaces. Contact electrification frequently involves two charged surfaces in close proximity. For contact electrification to occur, the surfaces are usually brought into contact and separated while being close to each other. One surface is charged positively, whereas the other surface is charged negatively. In this case, Paschen's law provides the framework for determining the dissipation of static charge from the two charged surfaces *via* dielectric breakdown of the gaseous atmosphere. The law is also applicable in other situations (*e.g.*, a flat grounded surface placed close to one charged surface). Paschen's law is given by eqn (5)

$$V_{\mathrm{b}} = \frac{B_{\mathrm{p}}pd}{\left\{\ln\left(A_{\mathrm{p}}pd\right) - \ln[\ln(1+\gamma_{\mathrm{SE}^{-1}})]\right\}} \tag{5}$$

where V_{b} is the breakdown voltage of a gas between two surfaces, p is the gas pressure, d is the gap distance between the two surfaces, A_{p} and B_{p} are gas-dependent constants, and γ_{SE} is the secondary electron emission coefficient.[90] The plot of V_{b} against pd is a "V" shaped curve (Fig. 4e), commonly referred to as Paschen's curve. It shows that the breakdown voltage is high at a small pd value, decreases at a moderate pd value, and increases again at a large pd value.[91]

An example that uses Paschen's law is the TENG device. In one study, the operation of the device involved two parallel surfaces repeatedly brought into contact and separated up to a maximum displacement, d, of 1 cm.[92] It was found that at $d =$ 1 cm, an increase in pressure from 1 atm to 5 atm increased the breakdown voltage, V_{b}, from 40 kV to 160 kV (Fig. 4f). The increase in breakdown voltage decreased the dissipation of static charge *via* dielectric breakdown of air. This reduction in charge dissipation allowed a correspondingly higher charge density to be generated on the surfaces, from 40 μC m^{-2} at 1 atm to 170 μC m^{-2} at 5 atm (Fig. 4g). The performance of the TENG device thus increased at higher air pressure: the maximum energy output per cycle increased from ~0.020 J at 1 atm to ~0.325 J at 5 atm. These results showed the importance of Paschen's law in designing devices for better performance.

3.1.4. "Contact de-electrification": dielectric breakdown between two contacting charged surfaces of the same polarity. Many industrial processes involve complex interactions among multiple materials (*e.g.*, the granular flow of particles). These interactions that involve frequent collision and separation of surfaces allow the materials to become highly charged *via* contact electrification. When two charged surfaces of the same polarity come into contact, they discharge *via* dielectric breakdown of the surrounding air in a process called contact de-electrification (Fig. 4h).[93,94]

For observing contact de-electrification, polymeric beads (nylon, Delrin, Torlon, and Teflon; $\frac{1}{4}$ inch in diameter) were first charged highly by contact electrification.[93] When the charged beads of the same polarity were brought into contact, the

charges of all contacted beads were found to decrease significantly. Based on the results of the simulation of the electric field, it was found that when charged beads of the same polarity were brought into contact, the electric field strength around the materials increased (Fig. 4i). When the strength of the electric field exceeds the dielectric breakdown strength of air, dissipation of static charge from the charged materials into the surrounding air occurs. This process thus causes the amount of charge of the charged materials to decrease *via* dielectric breakdown of air (*i.e.*, contact de-electrification). Therefore, the complexity of multiple interacting charged materials involves charge generation by contact electrification and charge dissipation by contact de-electrification.

3.1.5. Factors influencing charge dissipation *via* dielectric breakdown. The type of gas plays a key role in the dissipation of static charge by dielectric breakdown. Different gases have significantly different dielectric breakdown strengths. For example, the dielectric breakdown strength of air is 3.0 MV m^{-1}. Sulfur hexafluoride (SF_6), on the other hand, has a high dielectric breakdown strength of 7.7 MV m^{-1}. In comparison, argon has a low dielectric breakdown strength of 0.56 MV m^{-1} and helium has a low dielectric breakdown strength of 0.46 MV m^{-1}. Liquids and solids generally have very high breakdown strengths that are one or two orders of magnitude higher than that of gases. For example, distilled water breaks down at 65 MV m^{-1}, whereas glass breaks down at 200 MV m^{-1}.[95] Therefore, the dissipation of static charge generated by contact electrification is typically *via* dielectric breakdown of gas (*e.g.*, air), instead of *via* liquid and solid.

Different gases offer a wide range of dielectric breakdown strengths for various types of applications. For example, a typical TENG device requires the amount of static charge generated by contact electrification to be as large as possible for higher energy output.[92] In this case, it is advantageous to use SF_6 that has a high dielectric breakdown strength for reducing the dissipation of static charge due to the breakdown of the gas. A previous study reported that when the TENG device was in an atmosphere filled with SF_6 instead of air, the voltage of the device increased by 67% and the current increased by 180%.[96]

The humidity of the atmosphere affects the dielectric breakdown strength of air slightly. For a uniform electric field across a gap of 1.0 cm at 20 °C, it was observed that there was an increase of 5% in the dielectric breakdown strength of air when the relative humidity increased from 0 to 100%; hence, the amount of dissipation of static charge *via* dielectric breakdown of air decreased slightly with an increase in humidity.[97–99] This effect of humidity on the dissipation of static charge is thus opposite to that of surface conduction (*i.e.*, the extent of charge dissipation increases when the humidity is higher; see Section 5.2).

3.1.6. Dielectric breakdown is reversible. We previously found that the dissipation of static charge *via* dielectric breakdown of gas is surprisingly not only a purely dissipative process—the phenomenon is reversible. We observed the reversibility of the phenomenon by repeatedly changing the shape of a flexible material (Fig. 5a(i)).[100] Our experiments involved thin sheets of polytetrafluoroethylene (PTFE) that were prepared to have different initial shapes (*e.g.*, the extended sheet in state 1 shown in Fig. 5a(ii)). When the shape of the sheet of PTFE was changed (*e.g.*, the folded state 2 shown in Fig. 5a(ii)), we measured a continuous change in the amount of charge of the material (Fig. 5a(ii)). When the shape of the sheet was changed repeatedly (*e.g.*, between state 1 and state 2), we found that the amount of charge changed reversibly. We found that this continuously varying and reversible changes in charge were independent of the type of material, charging methods, initial shapes, transformations, and atmospheric conditions. A general result is that the materials tended to have higher amounts of charge in an extended state and lower amounts of charge in a compact shape. Because of the law of charge conservation, the difference in the amounts of charge of the material between these two states must be due to the migration of charge in and out of the material somehow in a reversible manner.

Fundamentally, we found from our experiments that the reversibility is due to the dynamic exchange of the charge of the material with the surrounding atmosphere. When the shape of the material changes from its initial extended state to a compact state, the charged surfaces of the material become closer. Results from our numerical simulation showed that the electric field strength around the surfaces increases when the material is more compact. This increase in electric field leads to the ionization of the air molecules. The ions that have the opposite polarity from that of the PTFE surface deposit onto the surface; this deposition leads to the decrease in the charge of the material. In other words, the charge of the material dissipates *via* dielectric breakdown into air. When the shape of the material is changed to become more extended, the electric field around the surface decreases correspondingly. In this state, the deposited ions desorb and leave the surface, thus allowing the charge of the material to increase and return to its original amount. These results thus showed that there is a fundamental relationship in electrostatics between the charge and the shape of the material.

We found that this reversibility of the dielectric breakdown can also be observed by changing the distance of separation between two charged surfaces (Fig. 5b(i)).[101] In these experiments, we used flat slabs of materials charged by contact electrification. The materials used included organic materials (*e.g.*, silicone rubber, natural rubber, Teflon, and low-density polyethylene) and inorganic materials (*e.g.*, glass, zirconium dioxide, and alumina). We brought the charged surfaces close to each other without any contact and measured their charges. We observed unexpectedly that the total charge was less than the sum of the individual charges of both the materials. When we repeatedly changed the distance of separation between the two charged surfaces (*i.e.*, repeatedly from far to close and from close to far), we discovered that the total charge of both the materials changed reversibly (Fig. 5b(ii)–(v)). We proposed that the mechanism of this reversibility is similar to the experiment in which the shape of the material is changed. The larger amount of charge at a larger distance corresponds to the extended state. Similarly, the lower amount of charge at a smaller distance corresponds to the compact state. In general,

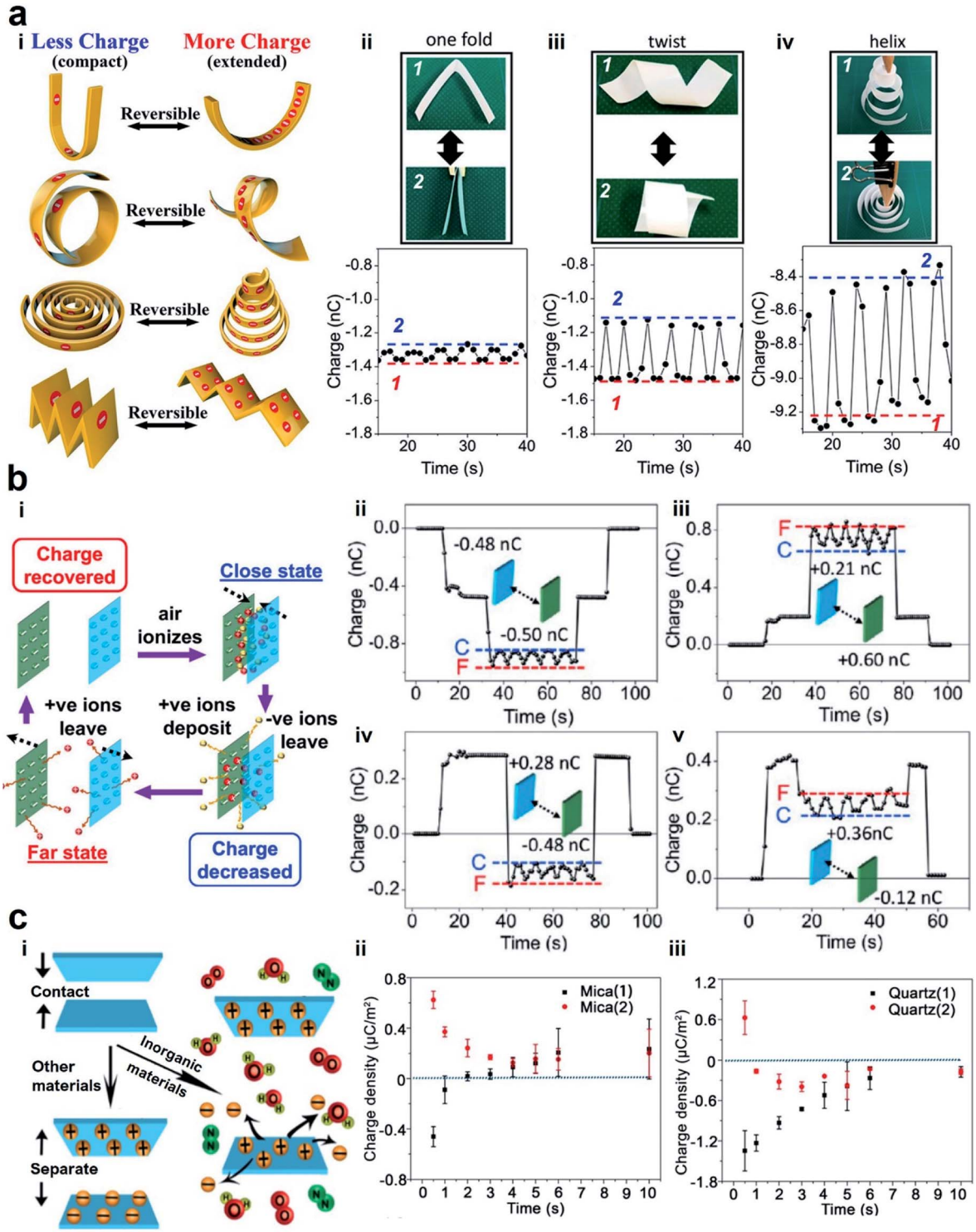

Fig. 5 Reversible charge dissipation into the gaseous atmosphere by dielectric breakdown. (a) Varying the shape of a material reversibly and continuously changes the amount of charge of the material. (i) Scheme illustrates the reversible changes of charge due to different shape transformations. (ii–iv) Images and plots of the changes in the shape (*i.e.*, between state (1) and state (2)) and the amounts of charge. Reproduced with permission (copyright 2020, American Chemical Society).[100] (b) Varying the distance of separation between two charged surfaces reversibly and continuously changes the amount of charge of the materials. (i) Scheme illustrates the mechanism of the reversible changes in charge due to the changes in the distance of separation. (ii–v) Reversible changes in charge between two surfaces that were charged with different polarities. State (C) represents the case when the surfaces were in proximity, whereas state (F) represents the case when the surfaces were far apart from each other. Reproduced with permission (copyright 2017, American Chemical Society).[101] (c) Anomalous change of charge that allows surfaces to charge with the same polarity after contact electrification. (i) Scheme illustrates the mechanism in which both surfaces are charged positively after contact. (ii and iii) Plots show the changes of charge over time after contact. Reproduced with permission (copyright 2018, American Chemical Society).[102]

these results showed that the phenomenon consists of two main parts: dissipation of static charge into the atmosphere *via* dielectric breakdown and regaining its original charge *via* the desorption of the ions deposited during the dielectric breakdown. This phenomenon thus allows the dielectric breakdown of air to occur reversibly.

One critical aspect of the two-part phenomenon is to determine whether ions within the atmosphere are indeed deposited onto the surfaces of materials after contact electrification (*i.e.*, desorption can only occur when there is deposition). In our previous study, we observed the deposition of ions from the surrounding atmosphere onto inorganic materials (Fig. 5c(i)).[102] Our experiments involved a variety of inorganic materials, such as mica, NaCl, Al_2O_3, $MgAl_2O_4$, silicon, ZnSe, KBr, quartz, and CaF_2. After charging the inorganic materials by contact electrification, we observed that the material discharged with time initially. However, after a short amount of time (~seconds), they seemed to gain charge of the opposite polarity (Fig. 5c(ii) and (iii)). This process of gaining charge indicated that ions from the surrounding atmosphere deposited onto the surfaces. Contact electrification typically gives rise to one positively charged surface and one negatively charged surface. On the other hand, this anomalous phenomenon that we observed unexpectedly gives rise to the same polarity of both the materials after contact electrification. For example, we showed that when mica was contact-charged with other inorganic materials (*e.g.*, NaCl, Al_2O_3, and KBr), both materials were always charged positively.

3.1.7. Applications of charge dissipation *via* dielectric breakdown. There are many interesting and practically useful applications based on the dissipation of static charge *via* the dielectric breakdown of the gaseous atmosphere. One application is the generation of negative ions for removing harmful atmospheric particulates *via* the dielectric breakdown of air.[103] The device consisted of a motion-simulated TENG and an array of carbon fiber (10 μm in diameter each). Operationally, the charge generated by the motion-simulated TENG was transferred into the carbon fibers (Fig. 6a). The sharp tips of the small carbon fibers promoted the creation of a high electric field. This high electric field ionized the surrounding air molecules and generated negative air ions (*e.g.*, O_4^-, OH^-, NO_2^-, and many others). A sealed container that contained smog particles was used to evaluate the effectiveness of the device. When the TENG was not in operation, it was visually observed that the smog particles remained suspended within the container after one minute (Fig. 6b). When the TENG was in operation, the smog particles were no longer visually observable within one minute (Fig. 6c). Measurements showed that the negative ions purified the PM 2.5 particles within the smog from 999 to 0 μg m^{-3} after approximately one minute. This result showed that the negative air ion generator removed atmospheric particulates effectively for sustainability and environmental protection.

Another fascinating application involves the ionization of gas molecules *via* dielectric breakdown for chemical analysis using a mass spectrometer.[104] Static charge was first generated on the inner surface of a silicone tube (inner diameter of 1 mm) by contact electrification of the inner surface (*i.e.*, *via* pressing the "pinch valve"; Fig. 6d). A vapor containing the analyte (*i.e.*, anisole) was passed through the tube and analyzed using a mass spectrometer. The results showed that the signal intensity of the analyte increased by 20 times when the inner surface of the tube was roughened ("After Rubbing" shown in Fig. 6e) *versus* when it was not roughened ("Before Rubbing" shown in Fig. 6e). The reason is that the increase in the surface roughness of the inner surface increased the generation of static charge by contact electrification. The increased amount of static charge enhanced the dielectric breakdown and ionization of the vapor molecules. This demonstration thus showed that contact electrification can be used for ionizing organic compounds for analysis by mass spectrometry (MS) instead of using the normal types of ionization sources. Results showed that a low concentration of 0.2 mg mL^{-1} of the analyte could be detected. This technology is thus useful for applications such as detecting trace amounts of volatile organic compounds.

Devices capable of collecting charge *via* dielectric breakdown are important for energy harvesting. An example is the direct-current TENG device (DC-TENG) for harvesting renewable energy from natural resources for powering calculators, charging capacitors,[105] and operating thermo-hygrometers.[106] In this device, there were three main components: (1) an upper copper surface (Cu(FE)), (2) a lower polymeric surface (PTFE), and (3) an additional metal plate attached on an acrylic stator as a charge collecting electrode (Cu(CCE)) (Fig. 6f).[105] When the upper surface slid across the lower surface, charge was generated on both surfaces. After sliding, the negative charge on the PTFE was exposed to the charge collecting electrode. The dielectric breakdown of the gas between the surface of the PTFE and the charge collecting electrode produced a current that flowed into an external circuit. The current produced from the DC-TENG was reported to be 0.4 μA in air and increased to more than 1 μA in oxygen (Fig. 6g). The lower dielectric breakdown strength of oxygen than air enabled the dielectric breakdown to be more effective, thus generating a larger current. The advantage of using DC-TENG over the typical alternating-current TENG (AC-TENG) is that DC-TENG can continuously produce unidirectional current without the need for a rectifier.[107]

3.2. Charge dissipation by disrupting co-localization of charge and radicals

Contact electrification of surfaces generally leads to both homolytic and heterolytic cleavages of molecular bonds on the surfaces. Heterolytic cleavage generates charge, whereas homolytic cleavage generates radicals.[108–112] Importantly, Grzybowski and co-workers found that the distribution of radicals and charges after contact electrification was not random—they were found to be co-localized within the same nanoscopic regions.[20] This co-localization of radicals and charges on a contact-charged surface of PDMS was observed directly by comparing the images obtained from Magnetic Force Microscopy (MFM) (*i.e.*, for visualizing the radicals) and KFM (*i.e.*, for visualizing the charges) (Fig. 7a). It was reported in the same study that the amount of charge generated decreased and the

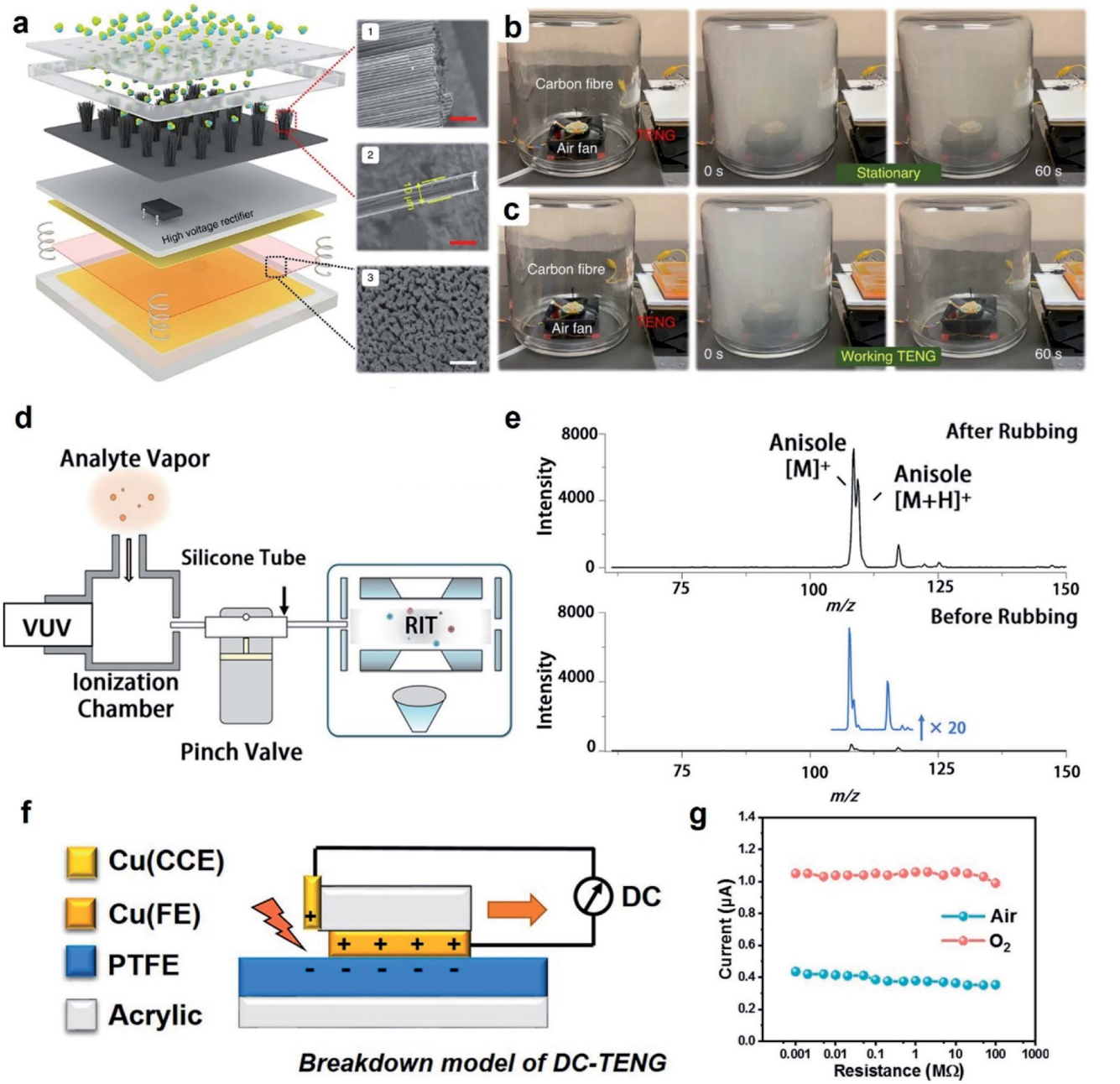

Fig. 6 Applications of charge dissipation into the gaseous atmosphere by dielectric breakdown. (a) Scheme illustrates a TENG device that generates negative ions *via* the dielectric breakdown of air for removing harmful atmospheric particulates. Clearance of smog when (b) the TENG device was not working and (c) when it was working. (a–c) Reproduced with permission (copyright 2021, Springer Nature).[103] (d) Scheme illustrates the ionization of gas molecules *via* dielectric breakdown for analysis by mass spectrometry (MS), and (e) analysis by MS showed the right signal detected for the analyte (anisole) when the tube was roughened for effective contact electrification ("After Rubbing"). The signal was weak (*i.e.*, by less than 20 times) when the tube was not roughened ("Before Rubbing"). (d and e) Reproduced with permission (copyright 2021, American Chemical Society).[104] (f) Scheme illustrates the operation of a DC-TENG (direct-current triboelectric nanogenerator), and (g) current obtained by the DC-TENG in air and oxygen (O_2) under atmospheric pressure. (f and g) Reproduced with permission (copyright 2021, Elsevier).[105]

rate of charge dissipation increased after doping small amounts of radical-scavenging molecules (*e.g.*, 2,2-diphenyl-1-picrylhydrazyl, DPPH or vitamin E) into PDMS. For example, doping the PDMS surface with 1 mM DPPH effectively increased the rate of charge dissipation from hours and days to merely a few minutes (Fig. 7b). Therefore, these results showed that the radicals that co-localized with the charges have a stabilizing effect on the charges. When the radical scavenger removes the radicals, the charge destabilizes and dissipates away rapidly.

The authors proposed that the stabilizing effect is due to the favorable interaction between the radical and the charge. The mechanoradicals generated by contact electrification can

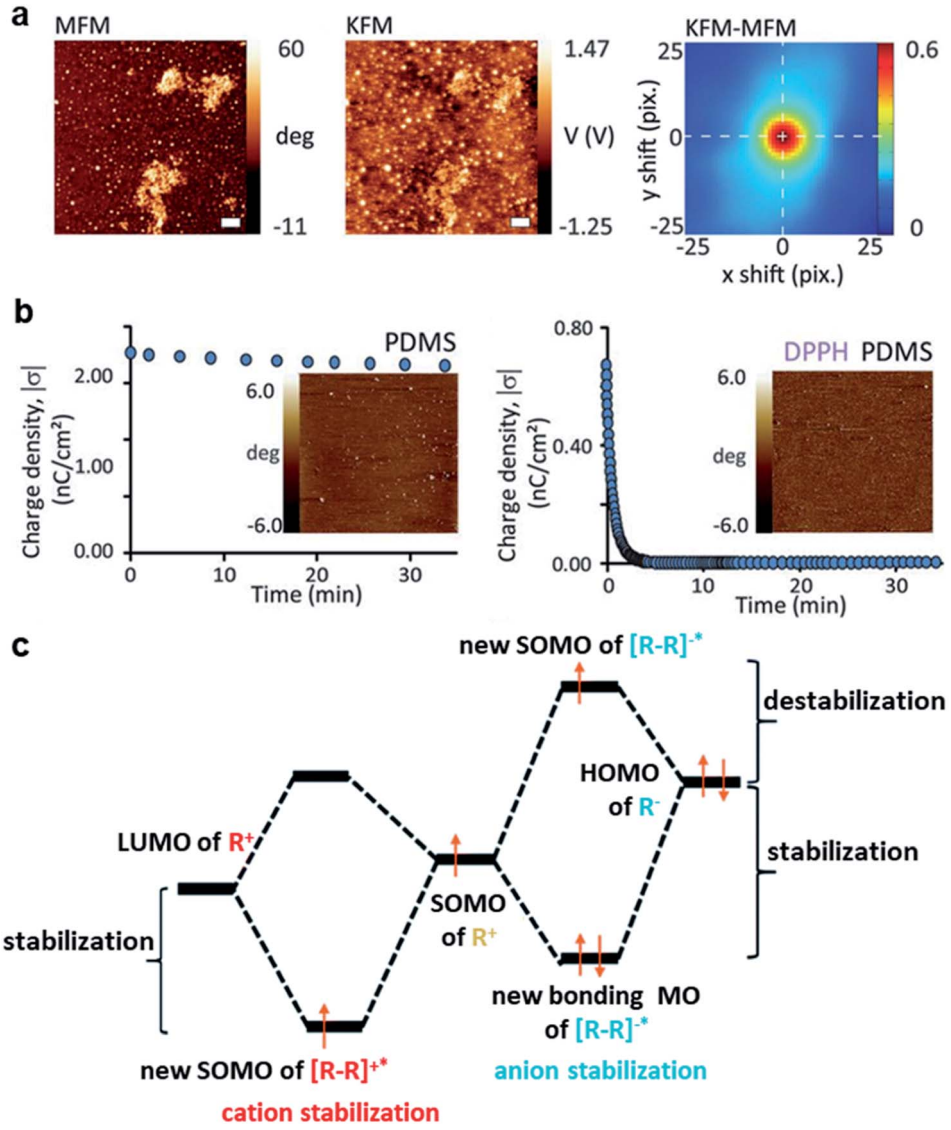

Fig. 7 Charge dissipation by removing the stabilizing radicals on the surface. (a) KFM and MFM images at the same location of a contact-charged surface of PDMS showing the co-localization of surface charge and radicals. (b) A surface doped with a radical scavenger (*i.e.*, DPPH; plot on the right) in PDMS dissipated charge much faster than the undoped surface of PDMS (plot on the left). (a and b) Reproduced with permission (copyright 2013, American Association for the Advancement of Science).[20] (c) Proposed mechanism of radicals stabilizing cations and anions, reproduced with permission (copyright 2017, Royal Society of Chemistry).[113]

stabilize the charge by forming an odd-electron bond between the molecular orbitals of the charged molecule and the radical. In the case of cations, a one-electron bond is formed between the lowest unoccupied molecular orbital (LUMO) of the cation and the singly occupied molecular orbital (SOMO) of the radical molecule. For the case of anion, a temporary three-electron bond is formed between the highest occupied molecular orbital (HOMO) of the anion and the SOMO of the radical. The removal of the radicals away from the ions by the radical scavenger destabilizes the ions, thus resulting in the faster dissipation of the ions from the surface (Fig. 7c).[113]

The increase in the rate of charge dissipation from the surface by the removal of radicals is a general phenomenon. Our group has developed a universal coating for minimizing the amount of static charge on surfaces by radical scavengers.[114] In this study, we dip-coated the surfaces of many types of materials, including metals, inorganic materials, and polymers, with two well-known radical scavengers, polydopamine (PDA) and tannic acid (TA). After contact-charging the coated materials with other materials (*e.g.*, PTFE and nylon), only relatively small amounts of charge were measured on the coated materials.

Radical scavengers that are present in nature prevent the build-up of static charge on surfaces. It was recently discovered by Baytekin and co-workers that the antistatic properties of wood were attributed to the radical-scavenging ability of lignin.[115] Wood samples with different lignin contents were charged by contact electrification using an aluminum (Al) surface. Results showed that the charge of the wood sample with lignin completely removed was 10 times higher than the charge of the natural wood sample (*i.e.*, with 32% lignin). In

addition, the rate of charge dissipation increased by two orders of magnitude by doping a piece of PDMS with only 5 wt% lignin.

3.3. Charge dissipation by deposition of atmospheric ions

Ions are naturally present in the atmosphere. The atmospheric ions (*i.e.*, both positive and negative) present at the ground level are produced mainly by cosmic rays and radioactive substances.[116] When a surface charged by contact electrification is exposed to the atmosphere, atmospheric ions of the opposite polarity with respect to the charged surface are attracted and deposited onto the surface. The deposition of the oppositely charged ions neutralizes the charge on the surface.

However, the concentration of atmospheric ions at the ground level is low under normal conditions. In most circumstances, the concentration of atmospheric ions ranges from one hundred to several thousand pairs per cubic centimeter.[117–119] This low concentration of air ions is unable to significantly dissipate charge generated by contact electrification on surfaces.

In a recent study, a conductive surface was charged *via* a high-voltage power supply to a surface potential of 2000 V (*i.e.*, an amount typically achievable by contact electrification between a conductor and an insulator).[120] The surface was either placed in cleanrooms with concentrations of the ions in the air of ~100–500 pairs per cm^3 or placed in a glove box with a concentration of the ions in the air of <10 pairs per cm^3. The dissipation of static charge from the surface was found to be on the order of 10 days in the cleanrooms and on the order of 40 days in the glove box. Hence, these results showed that although the dissipation of static charge *via* neutralization by atmospheric ions is very slow under normal conditions, a difference in the concentration of the ions in the air may cause a significant difference in the rate of charge dissipation.

On the other hand, the rate of charge dissipation can be greatly facilitated by introducing a high concentration of ions into the air surrounding the charged surface. High concentrations of ions can be generated by commercially available antistatic guns. They have been widely used for removing static charge on different types of materials (*e.g.*, plastics and inorganic materials) in households and laboratories. A typical antistatic gun consists of a trigger, a sharp conductive tip, and a piezoelectric crystal. When the piezoelectric crystal is pressed by pulling the trigger, positive ions are generated at the sharp tip. When the trigger is released, negative ions are generated. The released ions of the opposite polarity to the charged surface are attracted and deposited onto the surface, thus allowing the charge to dissipate rapidly away (*e.g.*, within seconds).

3.4. Back tunnelling and field emission

Quantum tunnelling is the phenomenon in which electrons penetrate through a potential energy barrier. A few groups have proposed that this phenomenon causes the dissipation of static charge generated during contact electrification by back tunnelling.[30,31,41] Specifically, the dissipation of static charge occurs when the surfaces are initially separated (*e.g.*, at a short distance of separation of ~1 nm) after the surfaces are brought into contact. At this point of initial separation, the electrons from the negatively charged surface undergo quantum tunnelling through the energy barrier to the positively charged surface. This process thus leads to the dissipation of the generated charge. The mechanism was reported to be significant for a surface charge density on the order of 10^{-3} C m^{-2} for the contact electrification between a metal and an insulator.[121]

When the distance of separation between the surfaces becomes larger than this short distance of a few nanometers (*i.e.*, for back tunnelling), electrons may be transferred between the surfaces by field emission. During separation, a high electric field is present between the oppositely charged surfaces. When the electric field is sufficiently high (*e.g.*, 10^9 V m^{-1}), electrons may be released from the negatively charged surface and transferred to the positively charged surface.[41]

3.5. Charge dissipation by thermionic emission

Thermionic emission is the release of electrons from a solid surface at sufficiently high temperature. Recent previous studies have found that the static charge on the surfaces of

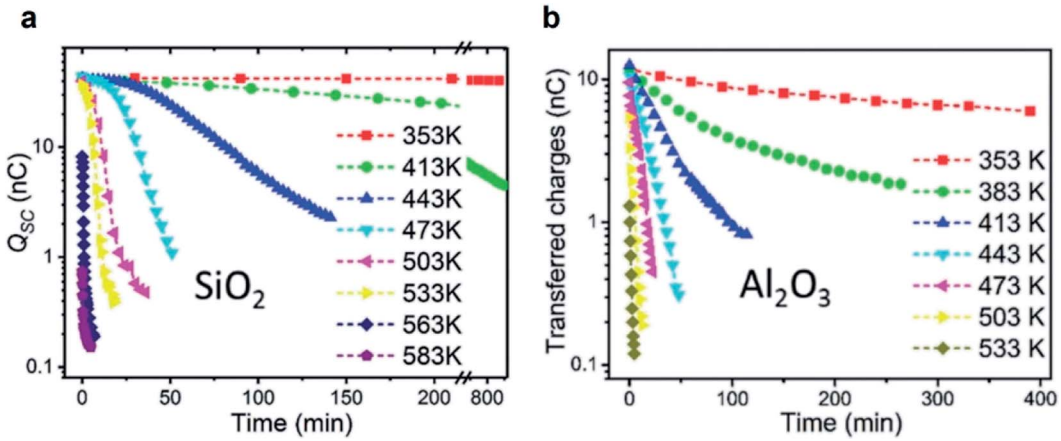

Fig. 8 Charge dissipation by thermionic emission. Amounts of static charge on (a) SiO_2 and (b) Al_2O_3 surfaces as a function of time under different temperatures. Reproduced with permission (copyright 2018, Wiley-VCH).[122]

silicon dioxide (SiO_2) and aluminum oxide (Al_2O_3) decayed rapidly at elevated temperatures (Fig. 8).[122] The oxides were first rubbed against polyurethane for gaining an initial charge density of 21.4 μC m^{-2} for SiO_2 and 6.7 μC m^{-2} for Al_2O_3. When heated up to 353 K, the charge on the surface of SiO_2 remained unchanged even after 800 min (Fig. 8a). When heated up to 583 K, however, the charge decayed to around zero after 5 min (Fig. 8b). The charge on the Al_2O_3 surface decayed to nearly zero at 533 K after 5 min. These results thus seem to indicate that the mechanism of charge dissipation is by thermionic emission.

4. Charge dissipation into liquid

4.1. Fundamentals of charge dissipation into liquid

The fundamental behaviors of static charge are generally not well understood. An important question involves what happens to the static charge (*i.e.*, generated by contact electrification) on a surface when it comes into contact with a liquid? To find out, we performed a series of experiments and found that the behavior of the static charge depends on a few factors.

In one study, we investigated the behavior of static charge on a surface when it comes into contact with water.[123] Our experiment involved first charging a piece of polyamide (nylon) highly positively (*i.e.*, by rubbing it against a piece of PTFE) or highly negatively (*i.e.*, by rubbing it against a piece of poly(ethylene glycol) diacrylate, PEGDA) (Fig. 9a). We then allowed a droplet of water (0.1 mL) to slide across the charged surface of nylon by gravity. After sliding, we found that the water droplet became charged to the same polarity as the highly charged surface. For example, the highly positively charged nylon of ~20 μC m^{-2} charged the droplet to a corresponding high positive charge of ~8 nC g^{-1}; the highly negatively charged nylon of ~−20 μC m^{-2} charged the droplet to a corresponding high negative charge of ~−4 nC g^{-1} (Fig. 9b). Hence, there was a transfer of charge from the highly charged surface to the water droplet—the static charge on the surface dissipated into the water upon contact. For some combinations of liquids and charged surfaces (*e.g.*, toluene and PTFE), the transfer was almost complete (*i.e.*, all the static charge on the surface readily transferred to the liquid).[124]

However, this direct transfer of charge from the charged surface to the liquid does not always occur. Examples include when the amount of charge on the surface is low or when other materials are used. In one experiment, we found that when water droplets slid across the surface of PTFE that was charged only slightly negatively (~−3 μC m^{-2}), the water droplets gained a positive charge instead (~3 nC g^{-1}) (Fig. 9c). As discussed previously in Section 2.2, contact electrification occurs when a water droplet flows across an initially uncharged PTFE surface; hence, water is expected to gain a positive charge after contact electrification with PTFE. There is thus a balance between charge generation and charge dissipation when a liquid flows across a charged surface. Charge dissipation dominates when a large amount of static charge is present on the charged surface. Charge generation, on the other hand, dominates when the amount of static charge is low, thus charging both the surface and the water.

Water is generally considered a conductive liquid for dissipating static charge. One initial expectation for the contact between a charged surface and an organic liquid—especially an electrically insulating nonpolar organic liquid—is that the static charge on the surface would not be disturbed by the liquid when in contact. Our experimental results, on the other hand, showed surprisingly that the charged surface was able to charge organic liquids—including nonpolar organic liquids—highly.[124] In this experiment, we allowed droplets of organic liquids (50 μL) to flow down surfaces charged by contact electrification. The organic liquids investigated included nonpolar organic liquids such as hexane, cyclohexane, 1,4-dioxane, *p*-xylene, *m*-xylene, toluene, ethylbenzene, *o*-xylene, diethyl ether, and chloroform. We found that the organic liquids gained large amounts of charge after flowing across the charged surfaces. For instance, the droplets that were in contact with the negatively charged surface gained charge on the order of −10 nC g^{-1}. These amounts of charge were comparable to the case when conductive water was charged by a high-voltage power supply to ~kilovolts. Notably, diethyl ether and chloroform droplets were charged far higher than water droplets charged to 4 kV (Fig. 9d). This result is surprising because there is currently no effective way to charge nonpolar organic liquids; not even a high-voltage power supply charges nonpolar organic liquids effectively. In general, our results showed that charge dissipation at the solid–liquid interface is a universal phenomenon for many types of solids and liquids that range from conductive water to highly insulating nonpolar organic liquids (*e.g.*, hexane).

4.2. Factors influencing charge dissipation into liquid

We found that the amount of static charge dissipated from a solid surface into liquid (*i.e.*, including water and organic liquids) is approximately linearly proportional to the amount of charge on the surface initially (Fig. 9b, c and e–g).[123,124] There are many ways by which the amount of static charge on the surface generated by contact electrification can be varied (*e.g.*, the method and pressure of contact). Hence, the corresponding amount of static charge dissipated into the liquid can be controlled *via* the many methods of charge generation of the surfaces.

Another important factor that influences the dissipation of static charge into liquid is the dielectric constant of the liquid. A higher dielectric constant of the liquid generally allows more static charge on the surface to dissipate into the liquid. An example involved a piece of PTFE that was charged to −4 nC and was immersed into either toluene or hexane. In this case, toluene acquired a charge of ~−4 nC (Fig. 9e), whereas hexane acquired only a charge of ~−2 nC (Fig. 9f). Because hexane had a lower dielectric constant than toluene, these results suggested that a liquid with a lower dielectric constant had a lower effectiveness of transferring charge from the solid to the liquid. In addition, another study also found that static charge on polymeric beads dissipated readily into a polar liquid.[125] The experiment involved immersing PTFE beads charged by contact electrification into a nonpolar solution that consisted of an organic solvent (hexane) and a photoexcitable dye (coumarin 6).

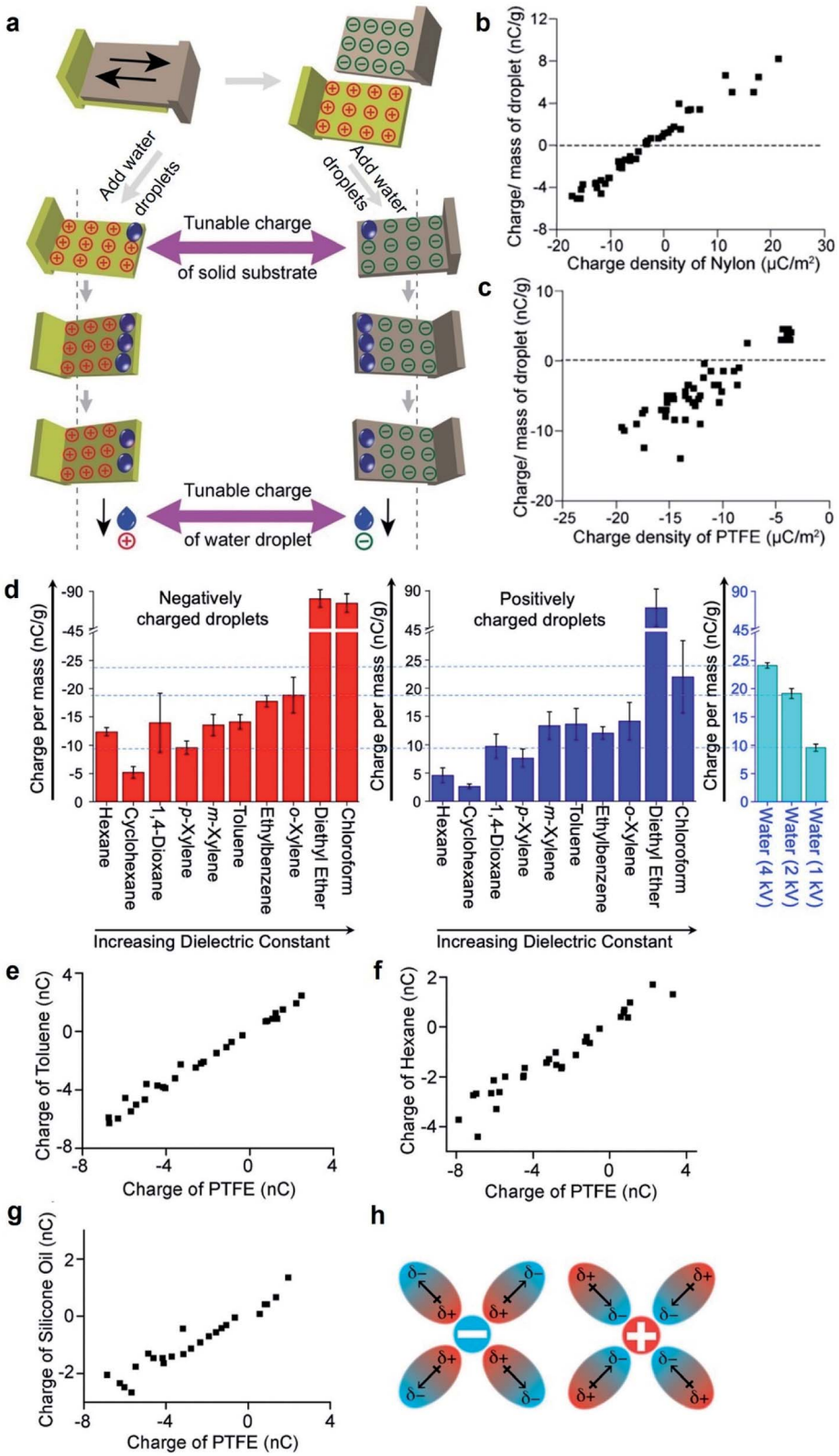

Fig. 9 Charge dissipation into liquid. (a) Dissipation of static charge from solid surfaces charged by contact electrification into water droplets. (b and c) Charge per unit mass of water droplets due to the dissipation of charge from surfaces against the initial charge density of (b) nylon and (c) PTFE. (a–c) Reproduced with permission (copyright 2016, Wiley-WCH).[123] (d) Charge per unit mass of organic liquids that were charged negatively (red bars; plot on the left) or positively (blue bars; plot in the middle) by the dissipation of charge from surfaces. Plot on the right shows the charge of water droplets that were charged to 1, 2, or 4 kV by a high-voltage power supply. (e–g) Charge of organic liquids (toluene, hexane, and silicone oil) against the initial charge of PTFE after the charged PTFE surface was immersed in the organic liquid. (h) Stabilization of charged species in organic liquid by the dipole of organic molecules. (d–h) Reproduced with permission (copyright 2020, American Chemical Society).[124]

The static charge on the PTFE beads was initially stable and able to be preserved for long periods of time (*e.g.*, hours to days). Upon UV radiation, coumarin 6 became polar and increased the overall polarity of the solution. In this case, the static charge on the PTFE beads was observed to dissipate into the solution faster (*e.g.*, tens of minutes). In general, these results suggested that liquids with a higher polarity gain more charge from the charged surface. Hence, it is possible that the fundamental mechanism may involve the stabilization of the charged species by the dipole of the organic molecules in the liquid (Fig. 9h).

The viscosity of the liquid may influence the solid–liquid dissipation of static charge.[124] For example, when a piece of PTFE that was charged to −4 nC was immersed into the highly viscous silicone oil, the oil was only able to charge to ∼−2 nC (Fig. 9g). This incomplete transfer of charge from the surface to the liquid suggested that a higher viscosity may prevent the effective circulation of the liquid around the surface for the transfer of charge, thus causing a lower effectiveness of the transfer.

4.3. Applications of charge dissipation into liquid

Because there are not many studies that investigated the charging of liquids by the transfer of static charge from surfaces, not many applications have been developed in this area. In particular, there were no applications developed for charged nonpolar organic liquids because there was no method that charged nonpolar organic liquids effectively. In our previous study, we used for the first time the dissipation of static charge into an organic pre-polymer mixture for fabricating permanently bulk-charged particles.[124] The fabrication involved the transfer of charge from a charged surface into the pre-polymer mixture and then polymerization of the charged mixture into polymeric silicone particles (∼500 μm to ∼5 mm). Our results showed that the charge was in the bulk volume of the particles as opposed to the typical surface-charged particles. The charge (∼0.02 to ∼5 nC) was stable for prolonged periods of time (∼months) and was not affected by the conditions of the surrounding liquid, including extreme pH values of 1 and 14. We further demonstrated the fabrication of particles that were both bulk-charged and bulk-magnetic. These particles could be manipulated flexibly *via* both magnetic and electric fields for applications (*e.g.*, biomedical applications).

In another application, we used the charged liquid generated by the solid–liquid charge dissipation and controlled the movement of the charged liquid *via* external electric fields.[123] For example, we manipulated the coalescence of two charged droplets for controlling chemical reactions. Another example involved varying the amount of charge in the liquid and the intensity of the external electric field for sorting and separation of the charged droplets (*e.g.*, for operations in microfluidic systems). We showed that we were able to effectively sort charged water droplets according to their polarity and amount of charge.

The charge on the solid surface was used to perform redox reactions (*i.e.*, "tribocatalysis"). A previous study reported that strontium titanate ($SrTiO_3$) nanofibers charged by contact electrification catalyzed the decomposition of the dye Rhodamine B (RhB).[126] The RhB solution with $SrTiO_3$ nanofibers was stirred continuously with a stir bar made of Teflon. Contact electrification between the Teflon rod and the nanofibers generated charged species on the nanofibers. This charged species then reacted with RhB and decomposed the molecules. It was found that the rate constant of decomposition at a stirring speed of 800 rpm was almost 8 times larger than that at a rate of 200 rpm. In a similar study, fluorinated ethylene propylene (FEP) powder charged by contact electrification was used to catalyze the degradation of methyl orange (MO).[16] Analysis by MS showed that the solution containing 5 ppm of MO solution completely degraded in the presence of 20 mg of FEP powder after 180 min.

The dissipation of charge from the surface to the liquid can be used to discharge any static charge present on solid surfaces. For example, a surface is usually immersed in either water or an organic liquid (*e.g.*, isopropyl alcohol) to remove any static charge from the surface.[114,127,128] This process is useful for many applications such as to mitigate the undesirable consequences of static charge and to perform controlled experiments in electrostatics.[114]

5. Charge dissipation into a solid

5.1. Bulk conduction

5.1.1. Fundamentals of bulk conduction. Bulk conduction is the mechanism by which static charge generated on the surface of a material by contact electrification is dissipated through the material to regions of lower electric potential (*e.g.*, to ground).[129] The effects of bulk conduction are commonly observed. For example, the mild electric shock experienced when touching a metal doorknob due to static charge as described in Section 3.1.1 is often the result of bulk conduction (*i.e.*, charge generated by contact electrification between the feet and the carpet is conducted to the hand; Fig. 10a). Similarly, when a person slides down a slide, charge is generated between the human body and the slide. The charge is then conducted through the body to the hair. Repulsion between the strands of charged hair causes the strands to stand on their ends (Fig. 10b). The effects of bulk conduction can also be demonstrated by a classic gold leaf electroscope that measures the amount of static charge on a conductor. The gold leaf electroscope consists of a metal ball attached to the top end of a metal rod, and two parallel strips of gold foil suspended from the bottom end of the rod (Fig. 10c). When a charged conductor is brought into contact with the metal ball, the charge is conducted through the metal ball and into both gold leaves *via* bulk conduction. As both gold leaves are charged with the same polarity, they repel each other. The amount of charge transferred from the charged surface to the electroscope can therefore be estimated from the amount of separation between the gold leaves. As bulk conduction is ubiquitous, it is an integral part in the understanding of the dissipation of static charge on solid surfaces.

5.1.2. Factors influencing charge dissipation *via* bulk conduction. Electrical conductivity is the property that

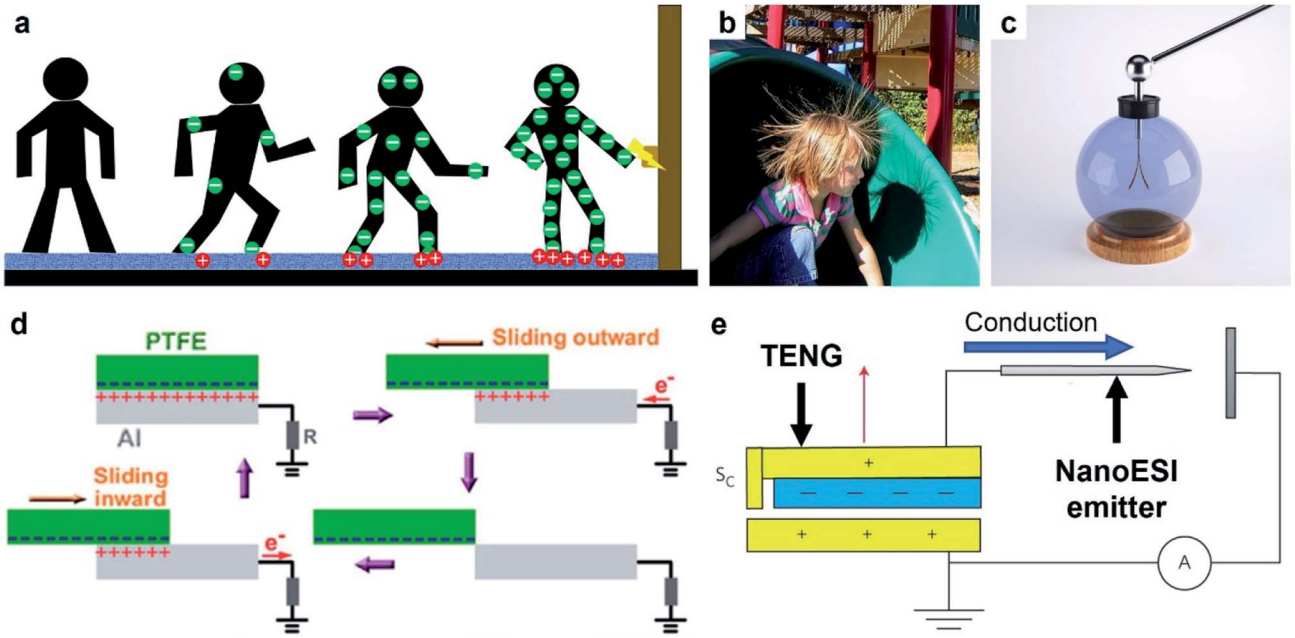

Fig. 10 Charge dissipation into a solid by bulk conduction. (a) Scheme illustrates the generation and conduction of static charge through a human body when a person walks across a carpet. Electric discharge (ESD) occurs when the person reaches for a metal doorknob due to the charge that migrated into the hands *via* bulk conduction. (b) Strands of hair repel each other after a child slides down a slide (Credits: Chris Darling/Wikimedia Commons). (c) Gold leaf electroscope (credits: haryigit/Shutterstock). (d) Scheme illustrates the operation of a typical TENG that uses bulk conduction for transferring power, reproduced with permission (copyright 2013, American Chemical Society).[154] (e) Scheme illustrates a TENG device that serves as the source of electrospray ionization and uses bulk conduction for concentrating the charge in the emitter, reproduced with permission (copyright 2017, Springer Nature).[156]

determines the dissipation of static charge generated by contact electrification *via* bulk conduction. Conductivity varies greatly depending on the material. Conductors have high conductivities typically due to the large number of mobile charge carriers (*e.g.*, electrons in metals) and partially overlapping conduction and valence bands. For example, metals have high conductivities typically on the order of 10^7 S m^{-1}.[95] Importantly, the human body is also a conductor due to the high conductivities of various parts of the body; for example, the conductivity of skin is 0.68 S m^{-1}, muscle is 1.18 S m^{-1}, fat is 0.041 S m^{-1}, and the brain is 0.59 S m^{-1}.[130] Therefore, static charge generated on one part of the human body spreads easily throughout the whole body. Insulators (*e.g.*, polymers and inorganic materials) have very low conductivities (10^{-20} to 10^{-10} S m^{-1}) due to the lack of mobile charge carriers and large band gaps (>4 eV).[131] The rate of charge dissipation through insulators is thus generally very slow; for example, the rate of dissipation through the bulk volume of fused quartz was estimated to be ~50 days. Semiconductors have moderate conductivities and small band gaps.[131,132]

A simple and common model for estimating the rate of charge dissipation through the bulk of materials is described as follows. The model involves a large flat slab of material (*i.e.*, with two large surfaces and a finite thickness). One surface of the material is charged by contact electrification, whereas the other surface is grounded. The electric field, E, between the charged surface and grounded surface (*i.e.*, *via* the bulk of the material) is described by the Gauss law as $E = \sigma/\varepsilon$, where σ is the charge density and ε is the permittivity of the material. From Ohm's law, the current density, J, due to charge dissipation is given by eqn (6)

$$J = E\gamma \tag{6}$$

where γ is the conductivity of the material. Combining the Gauss law and Ohm's law, we can arrive at eqn (7)

$$\sigma = \sigma_0 \, e^{-\frac{\gamma t}{\varepsilon}} \tag{7}$$

where σ_0 is the initial charge density and t is the time. The characteristic time of charge dissipation is hence $\tau = \varepsilon/\gamma$. This characteristic time is frequently used for determining the time of charge dissipation *via* bulk conduction for conductors and semiconductors.[133]

The rate of charge dissipation due to different conductivities of the materials is an important design consideration for applications. When it is necessary for the dissipation of static charge to be fast (*e.g.*, for preventing the undesirable consequences of static charge from occurring), conductors are used. Conversely, when it is necessary for the dissipation of static charge to be slow (*e.g.*, for storing charge for prolonged usage in applications), insulators are used.[133] In some situations, it is necessary to change the conductivity of a material.[134] For example, electrically insulating polymers (*e.g.*, rubbers) have excellent physical and chemical properties (*e.g.*, good flexibility, elasticity, and resistance to oxidation) that are desirable for many applications (*e.g.*, tires).[135,136] However, some applications

(*e.g.*, antistatic tires[137]) require fast dissipation of static charge away from these insulating polymers; hence, there is a need to increase the conductivities of these materials. Many different types of conductive additives have been developed for loading into polymers to improve their conductivities, including metallic particles,[138–140] conductive polymers (*e.g.*, polyaniline),[141] and conducting carbon derivatives (*e.g.*, carbon nanotubes,[137] carbon black,[142] carbon fibers,[143] graphite,[144] and reduced graphene oxide[145]). Through these methods, large increases in the rate of charge dissipation can be achieved for many practical applications related to contact electrification (*e.g.*, TENGs[146]).

In addition, there are many external factors that can influence the bulk conductivities of different types of materials. For example, the conductivity of metals usually decreases with increasing temperature.[95] The conductivity of semiconductors tends to increase with an increase in temperature or exposure to light.[147] This increase in conductivity is due to their small band gaps that allow excitation of electrons from the valence band to the conductive band. In addition, the conductivity of semiconductors can be increased by incorporating electron-rich (for n-type semiconductors) or electron-deficient (for p-type semiconductors) dopants.[148–151] The conductivity of semiconductors can also be influenced by the type of nanostructure in the materials.[152]

5.1.3. Applications of charge dissipation *via* bulk conduction. The three main categories of applications of charge dissipation *via* bulk conduction are fast dissipation by using materials with high conductivity for effective transferring of charge for applications, slow dissipation by using materials with low conductivity to retain charge for applications, and fast dissipation to prevent the undesirable effects of static charge.

5.1.3.1. Applications of bulk conduction. Bulk conduction allows the static charge generated on the surface by contact electrification to be channeled to another site for applications. For this type of applications, a high rate of charge dissipation *via* bulk conduction is needed. Countless applications require this transfer of charge; a few examples are discussed as follows.

Static charge generated on a surface can be converted to a source of electric current for applications *via* bulk conduction. This mode of operation is the basis of many TENG devices that harvest energy from human motions or natural sources for powering electronics, as described in Section 2.4.[153] A common setup consisted of a layer of PTFE and a grounded layer of Al (Fig. 10d).[154] First, static charge was generated on both layers by contact electrification when the layer of PTFE slid across the layer of Al. The static charge then produced a flow of current by quickly dissipating through the Al and into an external circuit. The high conductivity of Al facilitated a high rate of charge dissipation *via* bulk conduction. Repeated sliding of the two surfaces produced a maximum power density of 350 mW m^{-2} that was used directly to power 100 light-emitting diodes (LEDs).

In some cases, insulating materials with enhanced conductivities are required for applications. For example, a TENG can be made eco-friendly by using the biodegradable polylactic acid (PLA).[155] However, being an insulator, PLA is unable to dissipate charge *via* bulk conduction efficiently. By adding conductive graphene fillers into PLA, the resulting graphene–PLA composite was found to have a low volume resistivity of ~0.6 Ω cm. Due to the improved conductivity of the graphene–PLA composite, the static charge generated by contact electrification was able to dissipate rapidly though the bulk of the material and produce a peak power output of ~70 mW.

Two interesting applications involve the ionization of molecules (*e.g.*, in a liquid or gaseous medium) *via* bulk conduction of the static charge generated by contact electrification into a sharp tip. The first application involves the ionization of an analyte in a liquid medium for analysis by MS (Fig. 10e).[156] The static charge generated by contact electrification by a TENG device was conducted rapidly (*i.e.*, *via* bulk conduction) into a sharp tip; the high electric potential generated at the tip ionized the analyte. This TENG-powered nanoelectrospray ionization (TENG-nanoESI) was found to outperform the standard nanoESI in sensitivity when the concentration of the analyte sample was very dilute. For example, the TENG-nanoESI produced a detectable signal when analyzing a 10 pg mL^{-1} cocaine sample, whereas the standard nanoESI produced no detectable signal. The higher sensitivity of the TENG-nanoESI was proposed to be due to the higher open-circuit voltage of the TENG (5–9 kV) compared to that used in standard nanoESI (1–2 kV). The second application involves the ionization of air molecules for generating negative air ions as previously discussed in Section 3.1.7.[103] The operation of the device required the bulk conduction of the static charge generated by the TENG into the array of carbon fiber electrodes.

In some scenarios, the accumulation of static charge on a surface is useful for applications. Therefore, it is desirable to avoid bulk conduction by using insulating materials for the accumulation of charge. For example, in many TENG devices that use induction to produce an electric current, two insulating (polymeric) materials are used for contact electrification. In addition, the accumulation of stable amounts of static charge on surfaces produces electric fields that are useful in many applications. This general class of applications involving electric fields is described in more detail in Section 7.2.

5.1.3.2. Fast dissipation for preventing undesirable effects of static charge. The dissipation of static charge away from surfaces by bulk conduction is a common strategy used for preventing the undesirable effects of static charge from occurring. Many types of antistatic products based on charge dissipation *via* bulk conduction have been developed. For example, wrist straps with conductive wires are used to dissipate static charge on the human body (*e.g.*, hands) away for many industrial operations.[157] In particular, many sensitive electronic components are easily damaged by ESD (*e.g.*, *via* the charge on hands). For instance, a metal oxide semiconductor field-effect transistor (MOSFET) usually cannot withstand a potential of more than 250 V,[158] while the electrostatic potential in a human body is typically as high as thousands of volts.[157] Another example of a conductor-based antistatic product is the antistatic brush. Brushes made of conductive carbon fibers are able to dissipate the static charge on surfaces (*e.g.*, vinyl records) to remove dust

and other particulates. Other examples include antistatic shoes and antistatic carpets.

Besides conductors, many applications require the use of insulating materials added with conductive additives. For example, rubber is commonly used in car tires due to its superior elasticity and tensile strength. On the other hand, conductive additives are often doped into rubber to increase its conductivity to prevent potential electric shocks and sparks caused by static charge. A previous study reported incorporating multi-walled carbon nanotubes (MWCNTs) into the rubber matrix for fabricating anti-static tires.[137] At only 0.7 wt% of MWCNTs, the electrical resistance of the tire was found to be 10^5 Ω; thus, the conductivity of the material increased by four orders of magnitude compared to commercial tires (resistance $\sim 10^9$ Ω). The dispersed MWCNTs formed conductive pathways that dissipated charge generated by contact electrification between the tire and the road effectively.

5.2. Surface conduction

5.2.1. Fundamentals of surface conduction. Surface conduction is the lateral movement of charged species (*e.g.*, electrons or ions) across the surface of a material toward regions of lower electric potential. The charged species migrating through metals are electrons. For non-metals, the fundamental mechanism of surface conduction is poorly understood. Importantly, the identity of the charged species migrating across the surface (*i.e.*, in a dry environment)[42] and the depth of conduction within the surface of the material are unclear.[159,160] It is because of the complex chemical and physical composition of the surface. Surfaces usually include surface defects, varying physical roughness, adsorbed molecules (*e.g.*, water from the atmosphere), dangling bonds, and modifications of the surface due to reactions (*e.g.*, the formation of an oxidized layer on silicon that greatly reduces its surface conduction).[161]

Surface conduction is an important mechanism for the dissipation of static charge generated by contact electrification. A lack of surface conduction often causes many undesirable consequences that can be physically experienced or visually observed. A common example involves screens of computers that are covered with dust. As these surfaces are usually insulating, the contact electrification between the dust particles and the screen gives rise to an attractive electrostatic force that leads to the adhesion of the dust onto the screen (Fig. 11a). Due to the need to prevent the undesirable consequences of static charge (*e.g.*, electric shock and even explosion of flammable substances; Section 1), many commercial products have been developed and marketed for the purpose of dissipating static

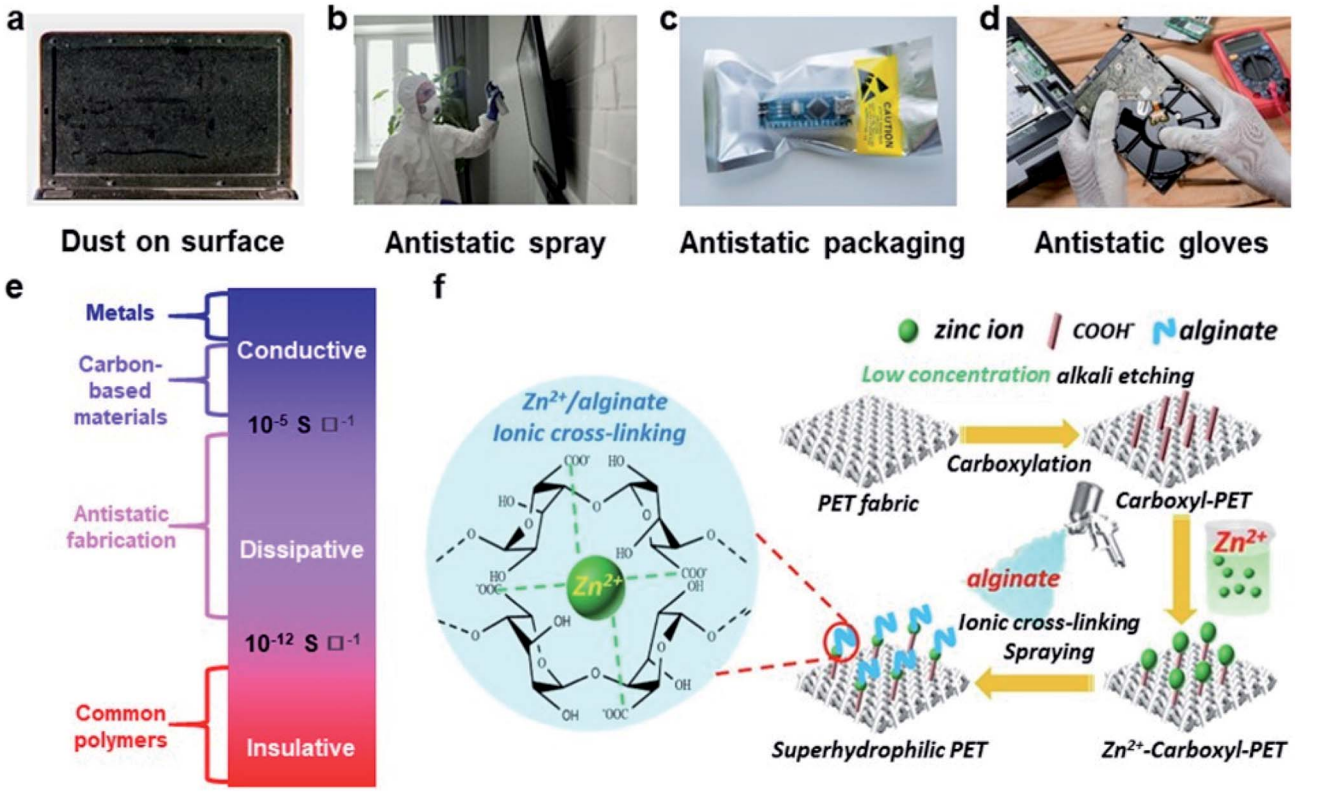

Fig. 11 Charge dissipation by surface conduction. (a–d) Common examples in daily life that involve surface conduction. (a) Adhesion of dust particles on a surface of a computer screen by electrostatic forces (credits: Ipek Morel/Shutterstock). (b) Applying antistatic spray on a screen to prevent dust adhesion (credits: Matilda Wormwood/Pexels). (c) Antistatic packaging for electronic components (credits: Igor Podgorny/Shutterstock). (d) Antistatic gloves for preventing ESD (credits: Nor Gal/Shutterstock). (e) Three regimes of charge dissipation *via* surface conduction. (f) Increasing hydrophilicity of PET fabric *via* layer-by-layer coating for improving surface conduction, reproduced with permission (copyright 2021, Elsevier).[190]

charge *via* surface conduction. One important product is the antistatic spray (Fig. 11b). When sprayed onto surfaces, the coating enhances surface conduction and eliminates the undesirable effects of static charge (*e.g.*, adhesion of dust onto surfaces). Other notable examples of commercial antistatic products that rely on enhancing surface conduction include antistatic gloves, antistatic packaging, antistatic clothing, and anti-dust screens (Fig. 11c and d).

5.2.2. Factors influencing charge dissipation *via* surface conduction. Different materials have different surface conductivities. For classifying the effectiveness of charge dissipation by surface conduction, materials of different surface conductivities are conventionally divided into three regimes (Fig. 11e). A material is considered conductive when its surface conductivity is higher than 10^{-5} S $\square^{-1}$. For example, surfaces covered with conductive coatings (*e.g.*, metallic or carbon-based materials) dissipate charge extremely rapidly (*i.e.*, characteristic time scale is usually in the range of 10^{-5} to 10^{-10} s); hence, static charge can hardly be detected on these surfaces. On the other hand, a material is considered insulative when its surface conductivity is lower than 10^{-12} S $\square^{-1}$. In general, common untreated polymers belong to this regime.[162–164] Insulative materials dissipate charge very slowly by surface conduction. For example, the characteristic time needed to dissipate charge by surface conduction for low density polyethylene (LDPE) and PTFE ranges from days to tens of days (*i.e.*, even when the dissipation of static charge was accelerated by providing sources of grounding at the edges of the surface).[165–168] A material is considered dissipative when its surface conductivity is in between those of conductive and insulative materials.

An important factor that greatly affects the surface conductivity of insulating surfaces is the adsorption of water from the atmosphere (*e.g.*, moisture due to a humid environment) onto the surfaces. Atmospheric water molecules are known to adsorb onto almost all types of surfaces, including even hydrophobic surfaces.[41,42] Water has a high conductivity of at least $\sim 10^{-5}$ S m^{-1} that is much higher than those of most polymers and non-conductive inorganic materials.[169] Ions in water serve as charge carriers that facilitate the fast dissipation of static charge. Previous studies found that the amount of adsorbed water on surfaces (including hydrophobic surfaces) was proportional to the humidity of the atmosphere.[23,161,170] Therefore, most insulating materials (*e.g.*, inorganic materials and polymers) showed a drastic increase in surface conductivity with increasing humidity.[161,171–174] For example, the surface conductivity of glass was found to be about 10^{-12} S $\square^{-1}$ below a relative humidity of 30%. Under these conditions, the glass belonged to the insulative regime. The characteristic time of charge dissipation was on the order of 100 seconds. When the humidity increased beyond 30%, the surface conductivity increased exponentially with increasing relative humidity. At a relative humidity of 80%, the surface conductivity was 10^{-8} S $\square^{-1}$. This increase of several orders of magnitude allowed the glass to undergo the transition from the insulative regime to the dissipative regime. The characteristic time of charge dissipation was less than 0.1 seconds in this case.[173]

Various functional relationships between humidity and surface conduction have been reported in previous studies. Some studies reported that the surface conductivity of insulating materials increased approximately exponentially with increasing humidity.[161,165] Other studies suggested that a threshold humidity was involved for other materials.[171,173,174] Below the threshold, the surface conductivity did not increase significantly as humidity increased; above the threshold, the surface conductivity increased drastically as humidity increased.

Many common strategies used in materials science can be used for increasing the surface conductivity of an insulating material. A common materials strategy for increasing surface conductivity is to enhance the intrinsic conductivity of the surface layer. Commonly used methods include doping the surface with conductive fillers[175–177] or coating with a conductive layer.[178–181] Materials such as metallic particles, carbon-based materials (*e.g.*, carbon nanotubes and graphene), and conductive polymers are frequently used.

Another common approach to increase surface conductivity is by increasing surface hydrophilicity. An increase in the hydrophilicity of a surface generally increases its hygroscopicity that leads to the adsorption of atmospheric water onto the surface. The adsorption of water allows the surface conductivity to increase. One frequently used method involves functionalizing surfaces with molecules that contain hydrophilic functional groups, including nitrogen-containing groups (*e.g.*, amine, amide, and ammonium), acidic functional groups (*e.g.*, carboxylic and sulfonic), and hydroxyl groups.[182–184] Another general method of increasing hydrophilicity involves treating the surface with high-energy sources such as plasma. This type of surface treatment gives rise to reactions of the surface with oxygen and water in the surrounding atmosphere. These reactions cause the formation of hydrophilic functional groups on the surface for increasing conductivity.[185–187]

Because of the complexity of the surface, it has been challenging to model the rate of charge dissipation by surface conduction. A very simple model is based on the same principles used for deriving the expression for the rate of charge dissipation by bulk conduction, except that the ground is provided at the lateral edge of the surface. Based on Ohm's law, the Gauss law, and the relationship between charge density and current density (see Section 5.1.2 for a similar derivation of the rate of charge dissipation by bulk conduction), the exponential decay of static charge is derived to be $\sigma \approx \sigma_0 e^{(-t/\tau)}$. For a 2D slab of material that has a length of $2L$ and a width of $2W$, the characteristic time constant of the rate of charge dissipation by surface conduction is $\tau_{2D} = (4\varepsilon(LW/(L+W))^2)/(\pi^2 d\gamma)$, where γ is the surface conductivity, d is the thickness of the material, and ε is the permittivity of the material. For a flat surface that is circular with a radius of R, the characteristic time constant is $\tau_{cylinder} = (0.17\varepsilon R^2)/d\gamma$.[188]

5.2.3. Applications of charge dissipation *via* surface conduction. Polyethylene terephthalate (PET) is one of the most common fabric materials (*i.e.*, for clothing) in the textile industry. PET accounts for more than 50% of the total fiber produced worldwide in 2021.[189] However, static charge

generates easily by contact electrification on clothing made of PET due to its low surface conductivity. The static charge generated due to the interaction between the human body and clothing (*e.g.*, when changing clothes) may cause ESD. ESD may cause the person wearing the clothing to experience mild electric shocks due to the static charge. More importantly, the ESD due to wearing the clothing made of PET may even pose the danger of fire or explosion in manufacturing facilities (*e.g.*, in petrochemical plants).

Therefore, it is important to devise ways to effectively dissipate static charge away from PET by surface conduction. One common strategy is to improve the hydrophilicity of PET. A previous study improved the surface conduction of PET fabric with layer-by-layer coating that involved crosslinking Zn^{2+} cations and alginate anions onto the surface of a carboxylated-PET fabric (Fig. 11f).[190] Results showed that the uncoated pristine PET fabric could be charged to a surface potential of 764 V, whereas the coated carboxylated-PET fabric could be charged to a surface potential of only 147 V. The half-life of the time needed for the dissipation of static charge on the surface of the uncoated pristine PET was 51 seconds, whereas the half-life of the time needed for the coated PET was only 0.08 seconds. The enhanced surface conduction of the coated PET was attributed to the hygroscopic nature of the coating. This coating led to the adsorption of additional layers of water on the surface. The adsorbed water on the surface increased the surface conductivity and rate of charge dissipation. Results from another study showed that the functionalization of the polymeric backbone of the PET fabric with Gemini quaternary ammonium salt and/or Gemini betaine increased its hydrophilicity significantly.[191] The increased hydrophilicity led to an increase in the surface conductivity of the fabric by 3 orders of magnitude.

Electronic components (*e.g.*, integrated circuits, ICs) contained within packaging materials are easily damaged by ESD. Non-conductive materials (*e.g.*, polycarbonate and polystyrene) have traditionally been commercialized as packaging materials. However, there is often frequent motion of the electronic component inside the packaging material when transported from one location to another. This motion causes repeated contact electrification between the electronic component and the packaging material, thus generating a large amount of static charge on the surfaces. ESD due to the accumulated charge then damages the IC chips easily. As a way to address this problem, manufacturers have fabricated conductive packaging materials (*e.g.*, based on carbon) for dissipating the static charge generated rapidly away. However, it is widely known that charge can still be generated on the IC chip by contact electrification between the packaging and the chip, thus causing damage to the IC chip. In addition, conductive materials greatly facilitate the conduction of charge from an external source (*e.g.*, the static charge on a human hand) into the interior of the package that damages the IC chip. Hence, the current strategy adopted in the market is to use a material that is in the dissipative regime (Fig. 11e). Commercialized dissipative packaging materials are developed using the methods discussed in the previous paragraphs (*e.g.*, coating a dissipative layer on the surface or doping the surface with conductive fillers). The moderate surface conductivity of dissipative materials helps in overcoming both the problems encountered by conductive and insulative materials: the charge generated by contact electrification can be dissipated away, whereas the conduction of charge from an external source into the interior of the package is limited. Therefore, dissipative packaging materials currently occupy a major share of the market. This development of packaging materials for electronic components shows the importance of carefully considering the dissipation of static charge by surface conduction for the design of products.

5.3. Material transfer for charge dissipation

We discussed that material transfer is a mechanism for the generation of charge by contact electrification (Section 2.1). In this section, we discuss that material transfer is also a mechanism for the dissipation of static charge. The reason is that the transfer of material may be bidirectional between the two surfaces undergoing repeated contact electrification; hence, material transfer may serve as the mechanism for both charge generation and charge dissipation.

When two uncharged surfaces are initially brought into contact and are then separated, charged fragments of the material of a specific polarity may transfer preferentially from one surface to another (Fig. 12a). Hence, one surface is charged positively and the other surface is charged negatively (*i.e.*, material transfer for charge generation). After many repeated contact and separation cycles, large amounts of positively charged fragments may accumulate on one surface, whereas large amounts of negatively charged fragments may accumulate on the other surface. A large number of charged fragments of a specific polarity on one surface give rise to the possibility that these charged fragments may transfer back to their original surface. This transfer of the charged fragments back to their original surface (*e.g.*, the positively charged fragments on the positively charged surface that transfer back to the negatively charged surface) thus causes the dissipation of static charge on both surfaces.

There is a lot of evidence for the transfer of fragments of the material from one surface to another for charge generation by contact electrification. The evidence includes the many direct observations *via* analytical techniques (*e.g.*, XPS and AFM) and the correlation between charge transfer and material transfer (Section 2.1). Due to the highly stochastic and varied nature of contact electrification, it is possible that the transfer of material is not strictly only from one surface to another—bidirectional transfer of materials between the surfaces may occur.

An important experimental observation that supports this bidirectional transfer of charged materials is the mosaic pattern of charge observed on contact-charged surfaces. Conceptually, the bidirectional transfer of charged materials should give rise to contact-charged surfaces with a distribution of positively charged and negatively charged regions on each surface. A previous study has reported that polymeric materials (*e.g.*, PDMS, PTFE, and polycarbonate, PC) showed nanoscale patches (or the mosaic pattern) of both positively and negatively charged regions located on the surfaces after contact electrification of

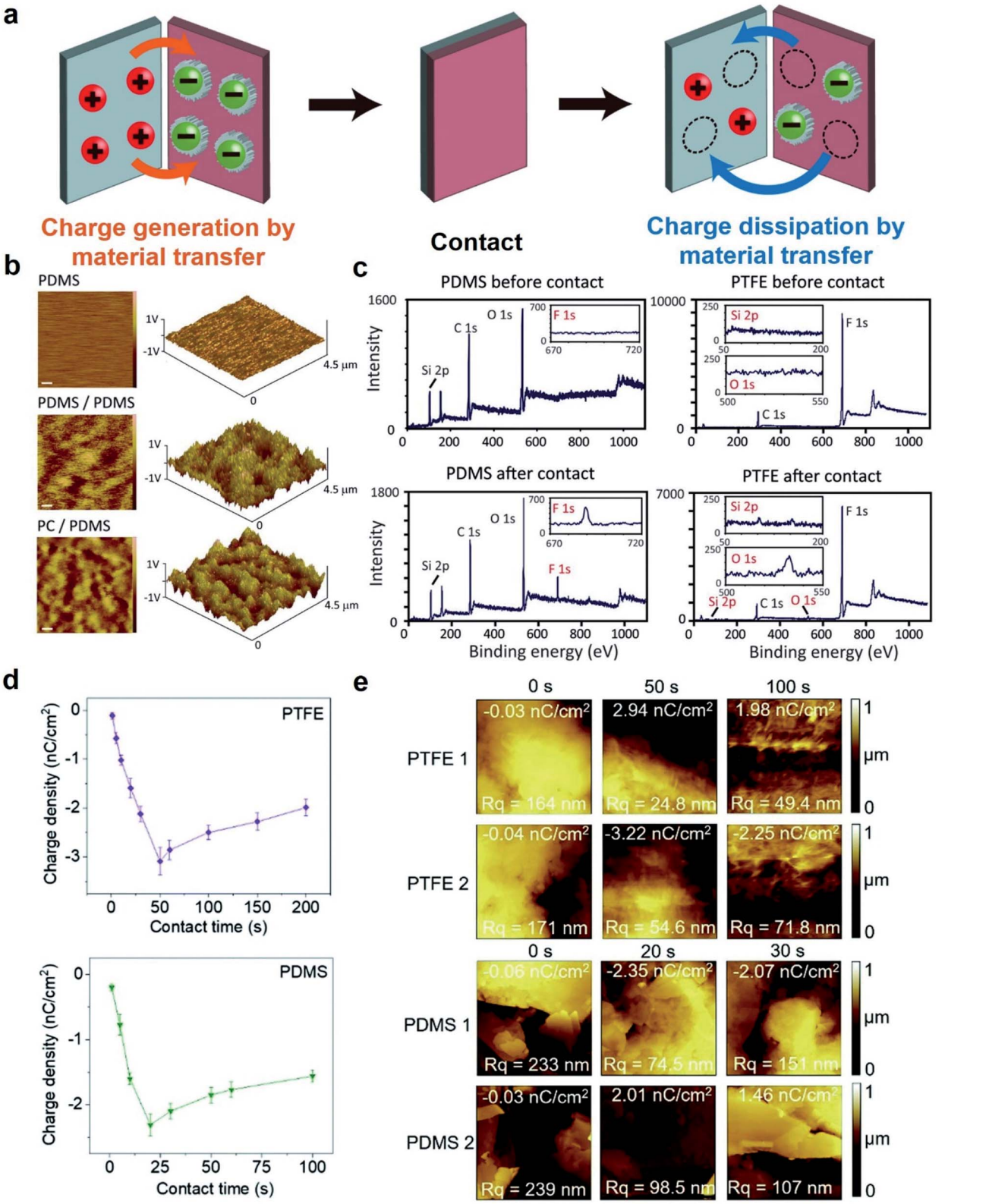

Fig. 12 Charge dissipation by material transfer at the solid–solid interface. (a) Scheme illustrates material transfer that leads to both charge generation and charge dissipation. (b) KFM images show the mosaic pattern of positively and negatively charged regions on a PDMS surface after contact electrification. (c) XPS analysis of PDMS and PTFE surfaces after contacting each other. (b and c) Reproduced with permission (copyright 2011, American Association for the Advancement of Science).[45] (d) Surface charge density and (e) AFM images of PTFE and PDMS surfaces after continuous contact electrification with the same material over time. (d and e) Reproduced with permission (copyright 2020, Royal Society of Chemistry).[192]

two materials by KFM (Fig. 12b).[45] The same study also reported that the transfer of materials was observed. Analyses (*i.e.*, *via* XPS and confocal Raman microscopy) of the surfaces of PDMS and PTFE after contact electrification showed that silicon was detected on PTFE and fluorine was detected on PDMS (Fig. 12c). Therefore, these results suggested that bidirectional material transfer occurred between the two surfaces.

Another study reported results that suggested the bidirectional transfer of materials by contact electrification.[192] The experiments involved the contact electrification of two flat slabs of polymers (*i.e.*, acetal, PTFE, PVC, PDMS, and nylon) of the same material. Initially, the materials had minimal amounts of charge (*i.e.*, <0.06 nC cm^{-2}) but had high surface roughnesses (*e.g.*, 170 nm for PTFE and 240 nm for PDMS) (Fig. 12d and e). After contact electrification of the materials by rubbing them for some time, the amounts of charge increased (*e.g.*, around −3.2 nC cm^{-2} for PTFE and −2.35 nC cm^{-2} for PDMS), but the surface roughnesses decreased (*e.g.*, 55 nm for PTFE and 100 nm for PDMS). As the differences in surface roughness may indicate the transfer of materials from one surface to another, this result suggested that material transfer may have caused the generation of charge by contact electrification. Subsequently, the contact electrification was performed for a longer period of time. The results showed that the amounts of charge decreased (*e.g.*, around −2.25 nC cm^{-2} for PTFE and −2.1 nC cm^{-2} for PDMS), but the surface roughnesses increased (*e.g.*, 72 nm for PTFE and 150 nm for PDMS). This result suggested that there was a transfer of materials in the opposite direction for decreasing the charge. In general, there seems to be an inverse relationship between the surface roughness and the amount of charge throughout the duration of contact electrification. This inverse relationship suggested that there is a bidirectional transfer of materials that influenced the amount of charge on the surfaces accordingly.

6. Summary of the mechanisms of charge dissipation

The previous sections discussed the different mechanisms of charge dissipation across all the interfaces of matter. We have summarized the characteristics of these mechanisms of charge dissipation in Table 1. The table lists the mechanisms, factors influencing the mechanisms, and correlations between the factors and the mechanisms. This table is thus a toolbox that enables researchers to design systems for achieving the desired rate of charge dissipation.

The dominant fundamental mechanism of charge dissipation is dictated by the actual circumstance. In the case of a grounded slab of a conductive metal, the dominant mechanism of charge dissipation (*i.e.*, among the other possible mechanisms of charge dissipation) is certainly the bulk conduction of static charge through the material into ground. For a non-conductive material in an environment with high humidity, surface conduction dominates. In a gaseous atmosphere that has a low dielectric breakdown strength, static charge is mainly dissipated *via* the dielectric breakdown of gas. In an atmosphere that has a sufficiently high concentration of ions (*e.g.*, ions released from an antistatic gun), the neutralization of static charge by the deposition of ions of the opposite polarity from the atmosphere is the dominant mechanism. A surface that contains radical-scavenging molecules readily dissipates static charge *via* disrupting the stable co-localization of charges and mechanoradicals on the surface. When a charged material is subjected to high temperatures, electrons are released from the surface *via* thermionic emission. When a charged surface is fully immersed in liquid, solid-to-liquid dissipation is the main mechanism of charge dissipation.

In many other cases, however, there is a high possibility that multiple mechanisms of charge dissipation occur simultaneously (*e.g.*, dielectric breakdown and surface conduction may occur at the same time after contact electrification).

7. Importance of differing rates of charge generation and charge dissipation

We have discussed the mechanisms of charge dissipation and strategies involved in achieving different rates of charge dissipation. Previously published studies have discussed the strategies of achieving different rates of charge generation by contact electrification. With the means of achieving different rates of charge dissipation and charge generation, we discuss in this section the importance of making use of these different rates for different circumstances and classes of applications. In the following sub-sections, we will discuss four specific cases: large generation and fast dissipation, large generation and slow dissipation, low generation and fast dissipation, and low generation and slow dissipation. We discuss that each of these cases has a greatly important fundamental rationale for performing their specific types of applications.

7.1. Large generation and fast dissipation

This first case involves implementing appropriate fundamental strategies for achieving the generation of large amounts of charge by contact electrification and fast release of the charge for various applications. By achieving large generation and fast dissipation of static charge, this case leads to large quantities of charge being supplied rapidly and dynamically into the surrounding medium. We divide the applications of this case into the three types of media: gas, liquid, and solid.

For supplying large quantities of charge rapidly into gas, one common way is to generate static charge by contact electrification and dissipate the charge by the dielectric breakdown of the gas (Section 3.1). We discussed the many important applications of this process in the section on dielectric breakdown; the applications include air ionizers,[103] MS,[104] DC-TENGs,[105] surface treatment,[83] and luminescence.[193] For example, the DC-TENG requires the generation of a large amount of static charge and fast dissipation *via* dielectric breakdown for producing an electric current that powers devices (Section 3.1.7).[105]

The second class of applications involves the rapid dissipation of large quantities of static charge into liquids. As discussed in Section 4.1, this process allows liquids to be charged

Table 1 Mechanisms, factors, and correlations of dissipation of static charge generated by contact electrification

Dissipation phase	Mechanism	Factor	Correlation	Ref.
Gas	Dielectric breakdown	Type of gas	Dielectric breakdown strength of gas correlates negatively with dissipation	96 and 105
		Pressure Gap distance	Product of pressure and the gap distance has a non-monotonic correlation with dissipation following Paschen's law	91
		Shape	A more compact shape induces dissipation (that is continuous and reversible when the shape is changed repeatedly)	100 and 101
		Humidity	Dissipation is slightly less at high humidity	97–99
	Disrupting the co-localization of charge and radicals	Concentration of the radical scavenger	Concentration of the radical scavenger correlates positively with dissipation	20 and 115
	Deposition of atmospheric ions	Concentration of atmospheric ions	Concentration of air ions correlates positively with dissipation	120
	Thermionic emission	Temperature	Temperature correlates positively with dissipation	122
Liquid	Charge transfer from the solid to the liquid phase	Charge on the solid surface	The solid–solid charge generation correlates positively with the amount of charge dissipated	123 and 124
		Polarity of the liquid	Dielectric constant correlates positively with the amount of charge dissipated	124 and 125
		Viscosity	Viscosity correlates negatively with the amount of charge dissipated	124
Solid	Bulk conduction	Conductivity	Conductivity correlates positively with dissipation	
		Permittivity	Permittivity of the solid correlates negatively with dissipation	133
		Concentration of the doped conductive material	Higher concentration of conductive dopants correlates positively with dissipation	137
		Temperature	Temperature correlates negatively with dissipation for metals; positively for semiconductors	95
	Surface conduction	Surface conductivity	Surface conductivity correlates positively with dissipation	
		Concentration of the doped conductive material on the surface	Higher concentration of conductive dopants on the surface correlates positively with dissipation	175–177
		Relative humidity	Humidity correlates positively with dissipation (especially non-conductors)	161 and 171–174
		Hydrophilicity	Hydrophilicity of the surface correlates positively with dissipation (especially non-conductors)	182–187

highly and quickly for important applications, such as sorting, manipulation, and controlled reactions. In particular, tribocatalysis requires the dissipation of a large amount of charge generated by contact electrification into the liquid medium for performing the reaction (Section 4.2).

The third class of applications involves the fast dissipation of large quantities of charge into a solid. In this case, a common route of dissipation is *via* bulk conduction. For example, energy can be harvested from natural sources by using TENG devices that use a metal electrode (Section 5.1.3).[194] The large generation of static charge and the fast dissipation *via* bulk conduction through the metal electrode allow as much electric current to be harvested as quickly as possible.

7.2. Large generation and slow dissipation

This combination of large generation by contact electrification and slow dissipation produces a large amount of charge that is stable over a long period of time. A large amount of stable charge produces a large stable electric field that is useful for many important applications *via* a number of modes of operations. The different modes of operation enabled by the large stable electric field include directing substances dynamically to specifically desired locations, separating substances of different polarities of charge, forming patterns *via* self-assembly, trapping of substances, and producing electricity.

The first mode of operation involves directing charged particles to specifically desired locations by an electric field for forming patterns. In electrophotography for the printing industry, toner particles are first charged by contact electrification.[195] An electric field then directs these charged toner particles systematically to specific locations on a surface for creating an image (*i.e.*, the desired pattern for printing onto a piece of paper). The large amount of charge generated on the particles and slow dissipation allow the toner particles to be stably charged during the process of directing them to their desired location. Another example involves the manipulation of droplets (*i.e.*, charged by a contact-charged surface; see Section 4.1) in multiphase microfluidic systems. Large amounts of stable charge in the droplets allow them to be flexibly guided by an external electric field toward any desired locations for different operations in the systems.[124]

The second mode of operation involves using a triboelectric separator that separates substances charged with different polarities by contact electrification.[196] When two types of polymeric particles are introduced into the separator, they collide among themselves and get charged by contact electrification. One type of polymeric particle is charged positively, whereas the other type of particle is charged negatively. The electric field applied within the separator then allows the differently charged particles to be separated according to their polarities. A large and stable charge on the particles is required for the separation to be achieved effectively.

The third mode of operation is based on using the large and stable charge of substances charged by contact electrification for pattern formation *via* self-assembly. It was reported in a study that by rolling two types of polymeric beads (*e.g.*, nylon and Teflon) in a vibrating container, the different types of beads were charged with different polarities.[197] Due to the electrostatic interactions among the differently charged beads, they were found to form different types of self-assembled patterns, including square, pentagonal, and hexagonal arrays. The formation of patterns due to the self-assembly allows large components to form ordered arrays easily (*e.g.*, for preparing micro-structured materials with specific properties). Large generation and slow dissipation of static charge is important to enhance the effectiveness of self-assembly.

The fourth mode of operation involves the trapping of harmful particles by electrostatic air filtering (Section 3.1.7).[198] The electric field produced by the charged layer (*i.e.*, charged by solid–solid contact electrification) within the triboelectric filter (*i.e.*, the face mask) attracts the air pollutant particles onto the charged layer, thus allowing clean air to pass through. A large and stable charged layer allows the filtering process to be effective over a long period of time.

The fifth mode of operation involves using the electric field generated on surfaces by contact electrification for powering devices (*i.e.*, *via* electrostatic induction). One main approach is by using TENG devices for energy harvesting (Section 2.1). The large amount of stable charge enables the TENG device to produce a large and sustained power[92] for applications such as motion sensors,[199] micromotors,[200] robotics,[201] self-powered systems,[202] implantable devices,[203] and many others.

7.3. Low generation and fast dissipation

This case involves minimizing charge generation by contact electrification and maximizing the rate of charge dissipation. This case is the ideal combination when static charge is undesirable and needs to be removed—the basis of antistatic surfaces. As discussed in the Introduction, antistatic surfaces are greatly needed in many activities in our daily lives and in almost all types of industries (*e.g.*, petrochemical, chemical, pharmaceutical, food, textile, automobile, construction, energy, electronics, semiconductor, and military industries). Static charge can reduce the efficiency of manufacturing processes (*e.g.*, due to fouling), decrease the quality of products (*e.g.*, due to contamination), damage equipment, and cause explosions. Therefore, this case is critically important for the preparation of antistatic surfaces for a vast range of circumstances and applications. The many strategies of fabricating antistatic surfaces have been discussed throughout the many sections of this perspective (see Sections 3.2, 5.1.3.2, and 5.2.3).

7.4. Low generation and slow dissipation

This case involves the generation of a regulated amount of charge and minimizing its dissipation from the surface. This case is useful in applications in which a moderate and sustained level of charge is important. Excessive amounts of charge generated by contact electrification are undesirable in many circumstances; importantly, static charge may cause ESD that damages the system or create an overly large electric field that has an adverse effect on the system.

One example involves a field effect transistor (FET) operated by a sliding-mode TENG device. One study described the design

of a tribotronic complementary inverter based on an n-type molybdenum disulfide (MoS_2) depletion mode FET and a p-type black phosphorus (BP) enhancement mode FET.[84] The sliding-mode TENG consisted of a top layer of PTFE and a grounded Al electrode. After sliding, a potential difference was created by the charged layer of PTFE due to contact electrification. This potential difference served as the gate voltage to control the current flow from the source to the drain of the transistor. The initial state of the TENG produced the "0" input (*i.e.*, no gate voltage); after sliding, the potential difference generated by the TENG produced the "1" input (*i.e.*, negative gate voltage). Slow dissipation of the static charge on the PTFE surface was needed to preserve the gate voltage at the desired level (~−15 V) for maintaining the "1" state for a sufficiently long period of time. A regulated amount of charge generation was needed to prevent the damage of the electronic component due to static charge (*i.e.*, ESD).[204] For example, a high applied gate voltage can cause gate oxide breakdown and the subsequent short through the insulating layer; this breakdown can cause a catastrophic failure of the device.[205] In general, this TENG device converts mechanical energy into electrical signals. The ability to control the logic device through external instructions has potential applications in mechanically controlled electronics, such as human–machine interfaces and motion-sensing devices.[206]

Another application of low charge generation and slow dissipation is in electrical stimulation for tissue regeneration. One study reported a self-activated bandage for electrotherapy that consisted of a TENG device connected to dressing electrodes.[80] This TENG-driven bandage was applied on rats (Fig. 13a). The TENG device harvested biomechanical energy from the motions of the rats (*e.g.*, breathing and movement of the muscles) and converted the energy into electrical pulses. The electrical pulses that flowed into the two dressing electrodes produced an electric field across the wound (Fig. 13b). In humans and animals, the endogenous electric field was observed to direct cell migration after injury.[207] Hence, this type of external electrical stimulation is similarly able to enhance wound healing by promoting cell migration, proliferation, and differentiation.[208] In the presence of the electric field generated by the TENG device, wound healing was accelerated in the direction of the electric field (Fig. 13c). The wound area was able to reach 94% closure within 48 h with the operation of the TENG device, whereas the wound area of the control group (*i.e.*, without the operation of the TENG) was 30% within 150 h. The slow dissipation of static charge allowed the electric field across the wound area to be sustained for the healing process. However, it was found in the same study that the electric field produced by the TENG device needed to be regulated. It was reported that exposure to excessively strong electric fields might

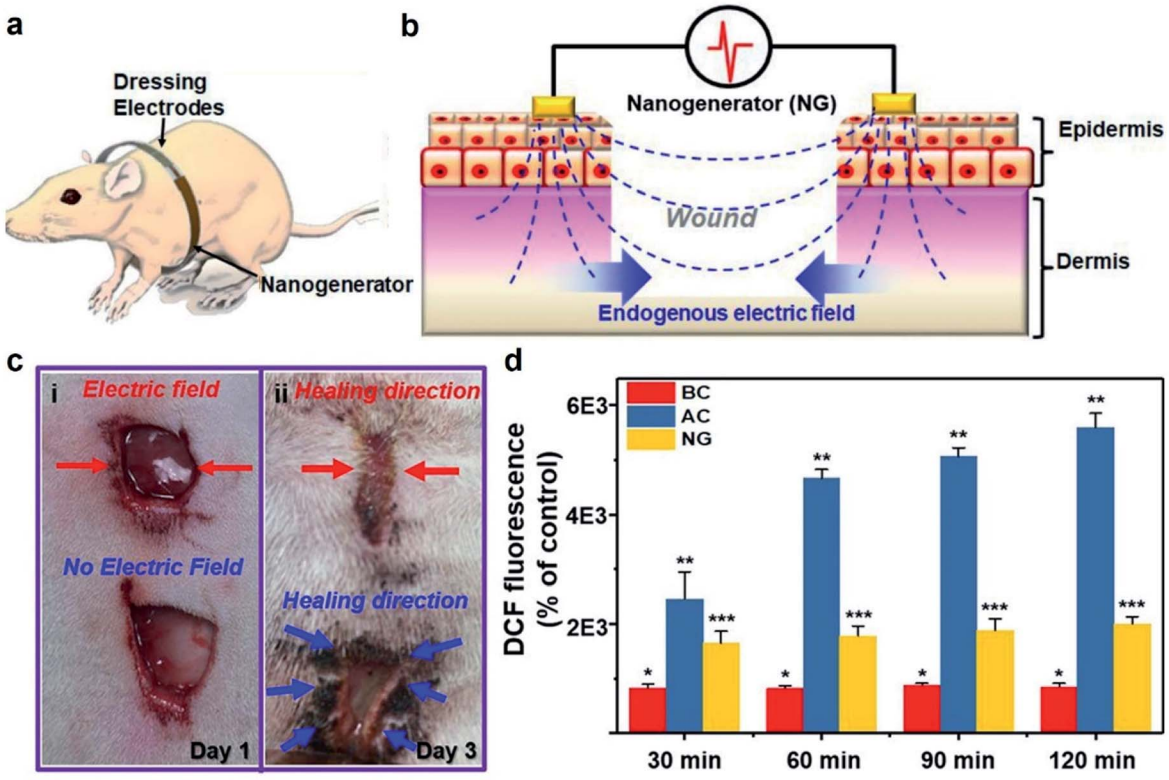

Fig. 13 Application of low generation and slow dissipation: self-activated electrotherapy bandage device. (a) TENG harvested biomechanical energy from the breathing of a rat. (b) Endogenous electric field generated by the wound healing device. (c) Digital image of a 3 day healing process with and without electric field stimulation. Directions of the electric field and healing are shown. (d) Dichlorodihydrofluorescein (DCF) fluorescence of a blank control (BC), stimulation *via* an alternating electric field generated by a function generator (AC), and stimulation *via* an electric field generated by a TENG (NG). Reproduced with permission (copyright 2018, American Chemical Society).[80]

induce harmful side effects, including the generation of reactive oxygen species (ROS) that could cause cell death.[209] Results showed that the electrical stimulation provided by the TENG device induced a 65% higher generation of ROS in the cell culture medium than that in the blank control groups (Fig. 13d). It is thus needed to carefully regulate the amount of electric field. A moderate amount of electric field is needed for accelerating the wound healing; on the other hand, any excessively large electric field due to the static charge generated by the TENG device causes harmful side effects.

8. Steady-state charge by balancing charge generation and charge dissipation

In this section, we discuss that the rates of charge generation and charge dissipation determine the amount of steady-state charge accumulated on a solid surface by contact electrification. The amount of steady-state charge is important in many applications and circumstances when the operation is continuously being performed. Importantly, we hypothesize that the same mechanism that underlies the generation of charge by contact electrification may give rise to the dissipation of charge as well for reaching the steady-state charge. Hence, whenever there is charge generation, there is charge dissipation due to the occurrence of the same fundamental mechanism. We discuss the process of achieving the steady-state charge in the two most common situations: the contact electrification between two solid surfaces in air and between a solid surface and a liquid.

The first case involves bringing two initially uncharged solid surfaces into contact and then separating them in air (Fig. 14a). During the initial contact, only charge generation occurs at the solid–solid interface. The mechanism may be due to electron transfer, ion transfer, and/or material transfer, as discussed in Section 2.1. After this initial contact, one surface gains a positive charge, and the other surface gains a negative charge (Fig. 14b). Once charge is present on the surfaces, charge dissipation occurs. Charge can dissipate into air (*e.g.*, by dielectric breakdown; Section 3) or solid (*e.g.*, by bulk and surface conduction;

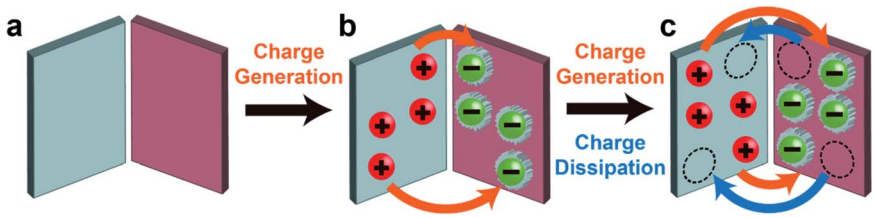

Fig. 14 Steady-state charge accumulated by the contact electrification of two solid surfaces in air. (a) Two uncharged surfaces before contact electrification. (b) The surfaces are charged by material transfer after initial contacts. (c) Steady-state charge achieved during contact electrification when charge is generated and dissipates simultaneously at the same rate *via* the same mechanism.

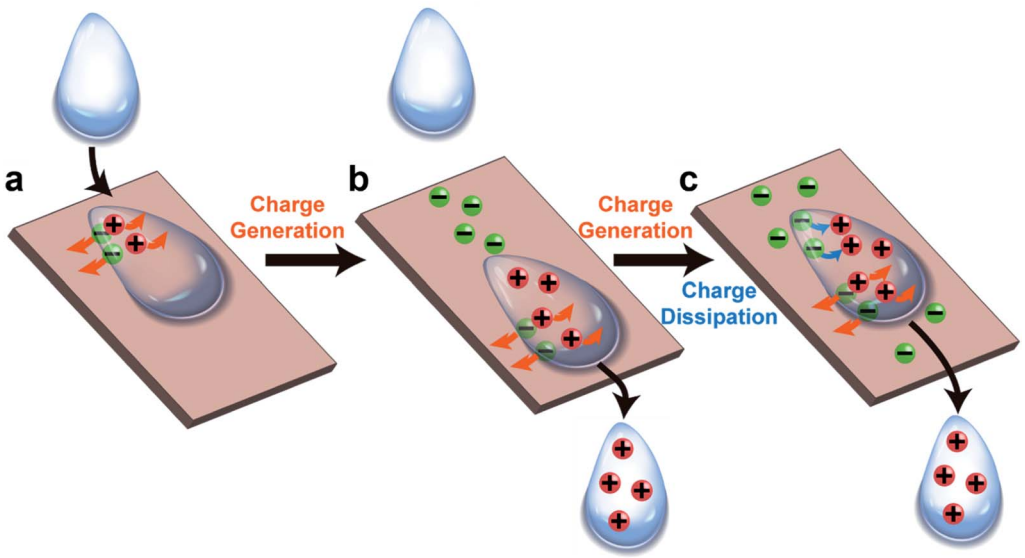

Fig. 15 Steady-state charge accumulated in the liquid by the contact electrification of a liquid droplet and a solid surface. (a) Charge separates at the solid–liquid interface when the liquid droplet comes into contact with the surface. (b) Charge is generated in the liquid droplet as it moves across the surface and leaves behind charge of the opposite polarity on the surface. Droplet is charged when it leaves the surface. (c) Case when subsequent liquid droplets come into contact with the surface. Steady-state charge is achieved when charge is generated and dissipates due to the recombination of charge at the solid–liquid interface.

Section 5) simultaneously. If the charge generation involves ion transfer and/or material transfer, charge dissipation may occur by the same mechanism. When ion and/or material transfer generates a large amount of positive charge on one surface and negative charge on the other surface with repeated contact electrification, back-transfer of the charged species (*e.g.*, ions or charged fragments of material) may occur (Section 5.3). The transfer of positively charged species back to the negatively charged surface causes the surfaces to discharge and *vice versa*. In this case, charge generation continues to occur as charge dissipation occurs simultaneously. A steady-state amount of charge is achieved when the rates of charge generation and charge dissipation are the same (Fig. 14c).

The second case involves bringing an initially uncharged droplet of liquid into contact with an initially uncharged solid surface and then removing the liquid away from the surface (*e.g.*, by sliding the droplet down the surface; Fig. 15a). When the liquid droplet first comes into contact with the solid surface, only charge generation occurs at the solid–liquid interface (Section 2.2). This separation of charge allows the solid surface and the liquid droplet to charge with opposite polarities (Fig. 15b). Once charge is present on the surface and in the liquid, charge dissipation occurs (*e.g.*, into the solid *via* bulk conduction). In particular, results from our group showed that a charged surface dissipates charge readily into the liquid (*i.e.*, including aqueous and organic liquids).[123,124] Therefore, in a continuous operation when multiple droplets flow across the surface, we believe that the charge on the surface generated by the solid–liquid contact electrification (*i.e.*, due to the passage of the previous droplets across the same surface) may dissipate back into the liquid. In this case, a steady-state amount of charge is achieved when the rates of charge generation and charge dissipation are balanced (Fig. 15c).

9. Conclusion

In this perspective, we highlighted the importance of charge dissipation—in most cases, charge generated by contact electrification dissipates easily and rapidly into any interface of matter. The importance of charge dissipation is shown from many points of view. First, charge dissipation is widespread: it is a class of phenomena that we frequently encounter in our daily lives (*e.g.*, dissipation of charge into the atmosphere *via* lightning and bulk conduction through our body for allowing strands of hair to stand on their own). Charge dissipation is already important in many applications developed in the field of electrostatics. Many technologies heavily rely on charge dissipation as the mechanism of operation regardless of whether they are developed many years ago (*e.g.*, antistatic spray for dissipating charge *via* surface conduction) or developed in recent research (*e.g.*, fabrication of permanently bulk-charged particles). Strong considerations of the rate of dissipation are often needed for the design of applications. For example, a fine balance between fast and slow rates of dissipation needs to be considered when designing the materials for electronic packaging. We discussed that there are many fundamental mechanisms that allow charge to dissipate readily and *via* different routes into different interfaces of matter.

In addition, we discussed that charge dissipation is not just a simple and straightforward fundamental mechanism that describes the loss of charge from a surface. It has been shown that charge dissipation is reversible (*i.e.*, for giving rise to the phenomenon that reversible changes in the shape lead to the corresponding changes in the charge of the material),[100,101] causes a nonlinear non-monotonic change in charge (*i.e.*, the anomalous phenomenon that switches the polarity of charge of the material during dissipation),[102] and influences the dynamics of multiple interacting charged particles (*i.e.*, contact de-electrification).[93,94] Hence, the mechanisms of dissipation can be fundamentally fascinating and lead to counter-intuitive outcomes.

Charge dissipation is critically important in determining the amount of steady-state charge developed during continuous operations that involve repeated contact electrification. Importantly, we discussed that charge dissipation severely limits the amount of charge that can be accumulated onto surfaces—dissipation becomes the dominant mechanism when the charge density of the surface is high. The amount of steady-state charge obtained by contact electrification is thus essentially a balance between charge generation and charge dissipation. We further discussed the importance of this balance in four extreme cases: large generation and fast dissipation, large generation and slow dissipation, low generation and fast dissipation, and low generation and slow dissipation. Each of this balance of dissipation and generation has its own purpose and class of important applications.

We made a hypothesis in this perspective about this balance that whenever there is generation, there is dissipation—*via* the same mechanism. At the solid–solid interface, the transfer of charge (*e.g.*, ion or material transfer) generates charge on the surface during the initial contacts; when the surfaces are sufficiently charged, the same mechanism of transfer of charge may plausibly occur in the opposite direction for the dissipation of charge. This bidirectional transfer of charge then allows the surfaces to reach a certain steady-state saturation of charge. A similar mechanism may occur at the solid–liquid interface when a solid surface charges against and dissipates into a moving liquid simultaneously.[59,123]

In general (similar to charge generation) much is still unknown about the mechanisms of the dissipation of charge in the field of contact electrification. A lot more investigations will be needed to understand the fundamentals and strategies for controlling the dissipation of charge better. A crucial aspect will be the ability to construct very well-controlled experiments for isolating an individual type of mechanism of dissipation. Isolating the specific mechanism allows it to be studied thoroughly and understood fully without the complications of the effects of other mechanisms of dissipation (*i.e.*, that may often occur simultaneously). A better understanding of the mechanisms of both charge generation and charge dissipation will enable us to obtain the desired level of steady-state charge for applications.

When compared to an electric current flowing through a conductive material (*e.g.*, a copper wire), the charge generated by contact electrification is relatively immobile on the surface. On the other hand, this perspective discussed the importance of charge dissipation: the ease and speed at which charge dissipates from the surface in most practical circumstances through all the interfaces of matter, including solid, liquid, and gas. In other words, charge is far from being immobile on surfaces regardless of the interface that the charged surface is in. This observation is well experienced around the world—charge when generated is expected to dissipate. Importantly, contact electrification mostly needs to be performed repeatedly and frequently throughout the entire time that the applications are required to be operated (*e.g.*, TENGs); if not for charge dissipation, the devices would need only the few initial contacts for generating the charge and operating the applications continuously over a significant amount of time. Therefore, the word "static" is a misnomer in most cases. "Static" is dynamic.

Conflicts of interest

There are no conflicts of interest to declare.

Acknowledgements

This work was financially supported by the Ministry of Education, Singapore, under grants R-279-000-576-114, R-279-000-633-114, and R-279-000-638-114, the Agency for Science, Technology and Research (A*STAR) under its AME Young Individual Research Grant Scheme (Project #A1884c0021), and the iHealthTech grant R-279-001-638-731.

References

1 Z. Quan, C. B. Han, T. Jiang and Z. L. Wang, *Adv. Energy Mater.*, 2016, **6**, 1501799.
2 D. Yoo, S.-C. Park, S. Lee, J.-Y. Sim, I. Song, D. Choi, H. Lim and D. S. Kim, *Nano Energy*, 2019, **57**, 424–431.
3 D. Jiang, F. Guo, M. Xu, J. Cai, S. Cong, M. Jia, G. Chen and Y. Song, *Nano Energy*, 2019, **58**, 842–851.
4 Z. L. Wang, *Nature*, 2017, **542**, 159–160.
5 M. Xu, P. Wang, Y. C. Wang, S. L. Zhang, A. C. Wang, C. Zhang, Z. Wang, X. Pan and Z. L. Wang, *Adv. Energy Mater.*, 2018, **8**, 1702432.
6 P. Maharjan, R. M. Toyabur and J. Y. Park, *Nano Energy*, 2018, **46**, 383–395.
7 J. Tian, F. Wang, Y. Ding, R. Lei, Y. Shi, X. Tao, S. Li, Y. Yang and X. Chen, *Research*, 2021, **2021**, 8564780.
8 M. S. Rasel, P. Maharjan, M. T. Rahman, M. Salauddin, S. M. S. Rana, S. Lee and J. Y. Park, *ACS Appl. Electron. Mater.*, 2021, **3**, 4376–4387.
9 S. Chen, N. Wu, L. Ma, S. Lin, F. Yuan, Z. Xu, W. Li, B. Wang and J. Zhou, *ACS Appl. Mater. Interfaces*, 2018, **10**, 3660–3667.
10 Z. Wang, T. Bu, Y. Li, D. Wei, B. Tao, Z. Yin, C. Zhang and H. Wu, *ACS Appl. Mater. Interfaces*, 2021, **13**, 56320–56328.
11 J. Chen, G. Zhu, J. Yang, Q. Jing, P. Bai, W. Yang, X. Qi, Y. Su and Z. L. Wang, *ACS Nano*, 2015, **9**, 105–116.
12 X. Pu, H. Guo, Q. Tang, J. Chen, L. Feng, G. Liu, X. Wang, Y. Xi, C. Hu and Z. L. Wang, *Nano Energy*, 2018, **54**, 453–460.
13 H. Guo, X. Pu, J. Chen, Y. Meng, M.-H. Yeh, G. Liu, Q. Tang, B. Chen, D. Liu, S. Qi, C. Wu, C. Hu, J. Wang and Z. L. Wang, *Sci. Rob.*, 2018, **3**, eaat2516.
14 C. B. Han, T. Jiang, C. Zhang, X. Li, C. Zhang, X. Cao and Z. L. Wang, *ACS Nano*, 2015, **9**, 12552–12561.
15 W. Lyskawinski, M. Baranski, C. Jedryczka, J. Mikolajewicz, R. Regulski, D. Rybarczyk and D. Sedziak, *Energies*, 2022, **15**, 19.
16 Z. Wang, A. Berbille, Y. Feng, S. Li, L. Zhu, W. Tang and Z. L. Wang, *Nat. Commun.*, 2022, **13**, 130.
17 X. J. Zhao, J. J. Tian, S. Y. Kuang, H. Ouyang, L. Yan, Z. L. Wang, Z. Li and G. Zhu, *Adv. Mater. Interfaces*, 2016, **3**, 1600187.
18 M. R. Maghami, H. Hizam, C. Gomes, M. A. Radzi, M. I. Rezadad and S. Hajighorbani, *Renewable Sustainable Energy Rev.*, 2016, **59**, 1307–1316.
19 S. Chattoraj, P. Daugherity, T. McDermott, A. Olsofsky, W. J. Roth and M. Tobyn, *J. Pharm. Sci.*, 2018, **107**, 2267–2282.
20 H. T. Baytekin, B. Baytekin, T. M. Hermans, B. Kowalczyk and B. A. Grzybowski, *Science*, 2013, **341**, 1368–1371.
21 J. Kemsley, *Chem. Eng. News*, 2016, **94**, 5.
22 Z. L. Wang, *Rep. Prog. Phys.*, 2021, **84**, 096502.
23 F. Galembeck, T. A. L. Burgo, L. B. S. Balestrin, R. F. Gouveia, C. A. Silva and A. Galembeck, *RSC Adv.*, 2014, **4**, 64280–64298.
24 L. Zhou, D. Liu, J. Wang and Z. L. Wang, *Friction*, 2020, **8**, 481–506.
25 R. D. I. G. Dharmasena and S. R. P. Silva, *Nano Energy*, 2019, **62**, 530–549.
26 H. Wang, L. Xu and Z. L. Wang, *Nanoenergy Adv.*, 2021, **1**, 32–57.
27 J. Wang, C. Wu, Y. Dai, Z. Zhao, A. Wang, T. Zhang and Z. L. Wang, *Nat. Commun.*, 2017, **8**, 88.
28 D. J. Lacks and T. Shinbrot, *Nat. Rev. Chem.*, 2019, **3**, 465–476.
29 J. Lowell, *J. Phys. D: Appl. Phys.*, 1975, **8**, 53–63.
30 W. R. Harper, *Contact and Frictional Electrification*, Laplacian Press, Morgan Hill, Calif., 1998.
31 J. Lowell and A. C. Rose-Innes, *Adv. Phys.*, 1980, **29**, 947–1023.
32 D. K. Davies, *J. Phys. D: Appl. Phys.*, 1969, **2**, 1533.
33 S. Lin, L. Xu, C. Xu, X. Chen, A. C. Wang, B. Zhang, P. Lin, Y. Yang, H. Zhao and Z. L. Wang, *Adv. Mater.*, 2019, **31**, 1808197.
34 B. A. Grzybowski, M. Fialkowski and J. A. Wiles, *J. Phys. Chem. B*, 2005, **109**, 20511–20515.
35 A. Wåhlin and G. Bäckström, *J. Appl. Phys.*, 1974, **45**, 2058–2064.
36 Z. L. Wang and A. C. Wang, *Mater. Today*, 2019, **30**, 34–51.
37 S. Lin, C. Xu, L. Xu and Z. L. Wang, *Adv. Funct. Mater.*, 2020, **30**, 1909724.

38 S. Lin, L. Xu, L. Zhu, X. Chen and Z. L. Wang, *Adv. Mater.*, 2019, **31**, 1901418.
39 L. S. McCarty, A. Winkleman and G. M. Whitesides, *J. Am. Chem. Soc.*, 2007, **129**, 4075–4088.
40 A. F. Diaz, D. Wollmann and D. Dreblow, *Chem. Mater.*, 1991, **3**, 997–999.
41 L. S. McCarty and G. M. Whitesides, *Angew. Chem., Int. Ed.*, 2008, **47**, 2188–2207.
42 C. A. Rezende, R. F. Gouveia, M. A. da Silva and F. Galembeck, *J. Phys.: Condens. Matter*, 2009, **21**, 263002.
43 X. Zhang, L. Chen, Y. Jiang, W. Lim and S. Soh, *Chem. Mater.*, 2019, **31**, 1473–1478.
44 W. R. Salaneck, A. Paton and D. T. Clark, *J. Appl. Phys.*, 1976, **47**, 144–147.
45 H. T. Baytekin, A. Z. Patashinski, M. Branicki, B. Baytekin, S. Soh and B. A. Grzybowski, *Science*, 2011, **333**, 308–312.
46 S. Piperno, H. Cohen, T. Bendikov, M. Lahav and I. Lubomirsky, *Angew. Chem., Int. Ed.*, 2011, **123**, 5772–5775.
47 H. T. Baytekin, B. Baytekin, J. T. Incorvati and B. A. Grzybowski, *Angew. Chem., Int. Ed.*, 2012, **51**, 4843–4847.
48 P. C. Sherrell, A. Sutka, N. A. Shepelin, L. Lapcinskis, O. Verners, L. Germane, M. Timusk, R. A. Fenati, K. Malnieks and A. V. Ellis, *ACS Appl. Mater. Interfaces*, 2021, **13**, 44935–44947.
49 R. K. Pandey, H. Kakehashi, H. Nakanishi and S. Soh, *J. Phys. Chem. C*, 2018, **122**, 16154–16160.
50 J. N. Israelachvili, *Intermolecular and Surface Forces*, Elsevier, Amsterdam, 2011.
51 R. Zimmermann, S. Dukhin and C. Werner, *J. Phys. Chem. B*, 2001, **105**, 8544–8549.
52 H. Kitabayashi, K. Tsuji and K. Itoh, *J. Electrost.*, 2005, **63**, 735–741.
53 J. Nie, Z. Ren, L. Xu, S. Lin, F. Zhan, X. Chen and Z. L. Wang, *Adv. Mater.*, 2020, **32**, 1905696.
54 S. Li, J. Nie, Y. Shi, X. Tao, F. Wang, J. Tian, S. Lin, X. Chen and Z. L. Wang, *Adv. Mater.*, 2020, **32**, 2001307.
55 S. Lin, L. Xu, A. Chi Wang and Z. L. Wang, *Nat. Commun.*, 2020, **11**, 399.
56 S. Lin, M. Zheng, J. Luo and Z. L. Wang, *ACS Nano*, 2020, **14**, 10733–10741.
57 J. Zhang, S. Lin, M. Zheng and Z. L. Wang, *ACS Nano*, 2021, **15**, 14830–14837.
58 S. Lin, X. Chen and Z. L. Wang, *Chem. Rev.*, 2022, **122**, 5209–5232.
59 Y. Sun, X. Huang and S. Soh, *Chem. Sci.*, 2015, **6**, 3347–3353.
60 N. Miljkovic, D. J. Preston, R. Enright and E. N. Wang, *Nat. Commun.*, 2013, **4**, 2517.
61 J. Nauruzbayeva, Z. Sun, A. Gallo, M. Ibrahim, J. C. Santamarina and H. Mishra, *Nat. Commun.*, 2020, **11**, 5285.
62 A. Z. Stetten, D. S. Golovko, S. A. L. Weber and H.-J. Butt, *Soft Matter*, 2019, **15**, 8667–8679.
63 M. D. Sosa, M. L. M. Ricci, L. L. Missoni, D. H. Murgida, A. Cánneva, N. B. D'Accorso and R. M. Negri, *Soft Matter*, 2020, **16**, 7040–7051.
64 W. Xu, H. Zheng, Y. Liu, X. Zhou, C. Zhang, Y. Song, X. Deng, M. Leung, Z. Yang, R. X. Xu, Z. Wang, X. C. Zeng and Z. L. Wang, *Nature*, 2020, **578**, 392–396.
65 X. Li, X. Ning, L. Li, X. Wang, B. Li, J. Li, J. Yin and W. Guo, *Nano Energy*, 2022, **92**, 106705.
66 H. Wu, N. Mendel, D. van den Ende, G. Zhou and F. Mugele, *Phys. Rev. Lett.*, 2020, **125**, 078301.
67 X. Li, J. Tao, X. Wang, J. Zhu, C. Pan and Z. L. Wang, *Adv. Energy Mater.*, 2018, **8**, 1800705.
68 Z. H. Lin, G. Cheng, S. Lee, K. C. Pradel and Z. L. Wang, *Adv. Mater.*, 2014, **26**, 4690–4696.
69 R. F. Gouveia and F. Galembeck, *J. Am. Chem. Soc.*, 2009, **131**, 11381–11386.
70 T. R. D. Ducati, L. H. Simoes and F. Galembeck, *Langmuir*, 2010, **26**, 13763–13766.
71 J. Fu, G. Xu, H. Wu, C. Li and Y. Zi, *Adv. Energy Sustainability Res.*, 2022, 2200051.
72 Z. Tang, S. Lin and Z. L. Wang, *Adv. Mater.*, 2021, **33**, 2102886.
73 X. Zhao, X. Lu, Q. Zheng, L. Fang, L. Zheng, X. Chen and Z. L. Wang, *Nano Energy*, 2021, **87**, 106191.
74 J. Nie, Z. Wang, Z. Ren, S. Li, X. Chen and Z. L. Wang, *Nat. Commun.*, 2019, **10**, 2264.
75 F.-R. Fan, Z.-Q. Tian and Z. L. Wang, *Nano Energy*, 2012, **1**, 328–334.
76 C. Rodrigues, A. Gomes, A. Ghosh, A. Pereira and J. Ventura, *Nano Energy*, 2019, **62**, 660–666.
77 S.-B. Jeon, D. Kim, G.-W. Yoon, J.-B. Yoon and Y.-K. Choi, *Nano Energy*, 2015, **12**, 636–645.
78 S. Wang, X. Mu, X. Wang, A. Y. Gu, Z. L. Wang and Y. Yang, *ACS Nano*, 2015, **9**, 9554–9563.
79 L. Xu, T. Jiang, P. Lin, J. J. Shao, C. He, W. Zhong, X. Y. Chen and Z. L. Wang, *ACS Nano*, 2018, **12**, 1849–1858.
80 Y. Long, H. Wei, J. Li, G. Yao, B. Yu, D. Ni, A. L. F. Gibson, X. Lan, Y. Jiang, W. Cai and X. Wang, *ACS Nano*, 2018, **12**, 12533–12540.
81 C. Zhao, H. Feng, L. Zhang, Z. Li, Y. Zou, P. Tan, H. Ouyang, D. Jiang, M. Yu, C. Wang, H. Li, L. Xu, W. Wei and Z. Li, *Adv. Funct. Mater.*, 2019, **29**, 1808640.
82 J. Nie, Z. Ren, J. Shao, C. Deng, L. Xu, X. Chen, M. Li and Z. L. Wang, *ACS Nano*, 2018, **12**, 1491–1499.
83 J. Cheng, W. Ding, Y. Zi, Y. Lu, L. Ji, F. Liu, C. Wu and Z. L. Wang, *Nat. Commun.*, 2018, **9**, 3733.
84 G. Gao, B. Wan, X. Liu, Q. Sun, X. Yang, L. Wang, C. Pan and Z. L. Wang, *Adv. Mater.*, 2018, **30**, 1705088.
85 D. Liu, L. Zhou, S. Li, Z. Zhao, X. Yin, Z. Yi, C. Zhang, X. Li, J. Wang and Z. L. Wang, *Adv. Mater. Technol.*, 2020, **5**, 2000289.
86 C. Helling, R. G. Harrison, F. Honary, D. A. Diver, K. Aplin, I. Dobbs-Dixon, U. Ebert, S.-i. Inutsuka, F. J. Gordillo-Vazquez and S. Littlefair, *Surv. Geophys*, 2016, **37**, 705–756.
87 J. Bendjamin, R. Thottappillil and V. Scuka, *J. Electrost.*, 1999, **46**, 259–269.
88 R. J. Van de Graaff, K. T. Compton and L. C. Van Atta, *Phys. Rev.*, 1933, **43**, 149–157.
89 J. J. Cole, C. R. Barry, X. Wang and H. O. Jacobs, *ACS Nano*, 2010, **4**, 7492–7498.

90 A. M. Loveless and A. L. Garner, *Phys. Plasmas*, 2017, **24**, 113522.
91 Y. Fu, P. Zhang, J. P. Verboncoeur and X. Wang, *Plasma Res. Express*, 2020, **2**, 013001.
92 Y. Zi, C. Wu, W. Ding and Z. L. Wang, *Adv. Funct. Mater.*, 2017, **27**, 1700049.
93 S. Soh, S. W. Kwok, H. Liu and G. M. Whitesides, *J. Am. Chem. Soc.*, 2012, **134**, 20151–20159.
94 S. Soh, H. Liu, R. Cademartiri, H. J. Yoon and G. M. Whitesides, *J. Am. Chem. Soc.*, 2014, **136**, 13348–13354.
95 D. R. Lide, *Handbook of Chemistry and Physics*, Taylor & Francis, 1997.
96 S. Lv, B. Yu, T. Huang, H. Yu, H. Wang, Q. Zhang and M. Zhu, *Nano Energy*, 2019, **55**, 463–469.
97 E. Kuffel, *Proc. Phys. Soc.*, 1959, **74**, 297.
98 A. N. Prasad and J. D. Craggs, *Proc. Phys. Soc.*, 1960, **76**, 223–232.
99 B. Li, X. Li, M. Fu, R. Zhuo and D. Wang, *J. Phys. D: Appl. Phys.*, 2018, **51**, 375201.
100 R. K. Pandey, C. K. Ao, W. Lim, Y. Sun, X. Di, H. Nakanishi and S. Soh, *ACS Cent. Sci.*, 2020, **6**, 704–714.
101 R. K. Pandey, Y. Sun, H. Nakanishi and S. Soh, *J. Phys. Chem. Lett.*, 2017, **8**, 6142–6147.
102 Y. Fang, L. Chen, Y. Sun, W. P. Yong and S. Soh, *J. Phys. Chem. C*, 2018, **122**, 11414–11421.
103 H. Guo, J. Chen, L. Wang, A. C. Wang, Y. Li, C. An, J.-H. He, C. Hu, V. K. S. Hsiao and Z. L. Wang, *Nat. Sustain.*, 2021, **4**, 147–153.
104 C. Xu, H. Ruan, W. Wang and H. Li, *Anal. Chem.*, 2021, **93**, 15897–15904.
105 Z. Yi, D. Liu, L. Zhou, S. Li, Z. Zhao, X. Li, Z. L. Wang and J. Wang, *Nano Energy*, 2021, **84**, 105864.
106 Z. Zhao, Y. Dai, D. Liu, L. Zhou, S. Li, Z. L. Wang and J. Wang, *Nat. Commun.*, 2020, **11**, 6186.
107 Y. Yang, H. Zhang and Z. L. Wang, *Adv. Funct. Mater.*, 2014, **24**, 3745–3750.
108 M. K. Beyer and H. Clausen-Schaumann, *Chem. Rev.*, 2005, **105**, 2921–2948.
109 R. S. Porter and A. Casale, *Polym. Eng. Sci.*, 1985, **25**, 129–156.
110 M. Sakaguchi, S. Shimada and H. Kashiwabara, *Macromolecules*, 1990, **23**, 5038–5040.
111 B. Baytekin, H. T. Baytekin and B. A. Grzybowski, *J. Am. Chem. Soc.*, 2012, **134**, 7223–7226.
112 L. Beraldo da Silveira Balestrin, D. Del Duque, D. Soares da Silva and F. Galembeck, *Faraday Discuss.*, 2014, **170**, 369–383.
113 T. Mazur and B. A. Grzybowski, *Chem. Sci.*, 2017, **8**, 2025–2032.
114 Y. Fang, S. Gonuguntla and S. Soh, *ACS Appl. Mater. Interfaces*, 2017, **9**, 32220–32226.
115 M. Özel, F. Demir, A. Aikebaier, J. Kwiczak-Yiğitbaşı, H. T. Baytekin and B. Baytekin, *Chem. Mater.*, 2020, **32**, 7438–7444.
116 R. G. Harrison and K. S. Carslaw, *Rev. Geophys.*, 2003, **41**, 1012.
117 N. S. Shuman, D. E. Hunton and A. A. Viggiano, *Chem. Rev.*, 2015, **115**, 4542–4570.
118 X. Ling, R. Jayaratne and L. Morawska, *Atmos. Environ.*, 2010, **44**, 2186–2193.
119 H. Tammet, U. Horrak, L. Laakso and M. Kulmala, *Atmos. Chem. Phys.*, 2006, **6**, 3377–3390.
120 C. Heinert, R. M. Sankaran and D. J. Lacks, *J. Electrost.*, 2022, **115**, 103663.
121 J. Lowell, *J. Phys. D: Appl. Phys.*, 1979, **12**, 1541.
122 C. Xu, Y. Zi, A. C. Wang, H. Zou, Y. Dai, X. He, P. Wang, Y. C. Wang, P. Feng, D. Li and Z. L. Wang, *Adv. Mater.*, 2018, **30**, 1706790.
123 Y. Sun, X. Huang and S. Soh, *Angew. Chem., Int. Ed.*, 2016, **55**, 9956–9960.
124 K. H. Lim, Y. Sun, W. C. Lim and S. Soh, *J. Am. Chem. Soc.*, 2020, **142**, 21004–21016.
125 S. D. Cezan, A. A. Nalbant, M. Buyuktemiz, Y. Dede, H. T. Baytekin and B. Baytekin, *Nat. Commun.*, 2019, **10**, 276.
126 J. Cao, Y. Jia, X. Wan, B. Li, Y. Zhang, S. Huang, H. Yang, G. Yuan, G. Li, X. Cui and Z. Wu, *Ceram. Int.*, 2022, **48**, 9651–9657.
127 T. Ohmi, S. Sudoh and H. Mishima, *IEEE Trans. Semicond. Manuf.*, 1994, **7**, 440–446.
128 K. Sayfidinov, S. D. Cezan, B. Baytekin and H. T. Baytekin, *Sci. Adv.*, 2018, **4**, eaau3808.
129 J. Kindersberger and C. Lederle, *IEEE Trans. Dielectr. Electr. Insul.*, 2008, **15**, 941–948.
130 A. Ibraheem and M. Manteghi, *Prog. Electromagn. Res.*, 2014, **145**, 195–202.
131 W. H. Strehlow and E. L. Cook, *J. Phys. Chem. Ref. Data*, 1973, **2**, 163–200.
132 G. Wu, R. Liang, M. Ge, G. Sun, Y. Zhang and G. Xing, *Adv. Mater.*, 2022, **34**, 2105635.
133 N. Jonassen, *Electrostatics*, Springer Science & Business Media, 2013.
134 C. Cao, F. Liang, W. Zhang, H. Liu, H. Liu, H. Zhang, J. Mao, Y. Zhang, Y. Feng, X. Yao, M. Ge and Y. Tang, *Small*, 2021, **17**, 2102233.
135 L. Mirizzi, M. Carnevale, M. D'Arienzo, C. Milanese, B. Di Credico, S. Mostoni and R. Scotti, *Molecules*, 2021, **26**, 3555.
136 K. Evans, *Mater. Des.*, 1984, **5**, 43–45.
137 Y. Lu, J. Liu, G. Hou, J. Ma, W. Wang, F. Wei and L. Zhang, *Compos. Sci. Technol.*, 2016, **137**, 94–101.
138 D. Yang, Y. Ni, Y. Liang, B. Li, H. Ma and L. Zhang, *Compos. Sci. Technol.*, 2019, **180**, 86–93.
139 A. Krainoi, C. Kummerlöwe, N. Vennemann, Y. Nakaramontri, S. Pichaiyut and C. Nakason, *J. Appl. Polym. Sci.*, 2019, **136**, 47281.
140 M. Wang, Y. Feng, Y. Zhang, S. Li, M. Wu, L. Xue, J. Zhao, W. Zhang, M. Ge, Y. Lai and J. Mi, *Appl. Surf. Sci.*, 2022, **596**, 153582.
141 B. D. Malhotra, S. Ghosh and R. Chandra, *J. Appl. Polym. Sci.*, 1990, **40**, 1049–1052.
142 R. A. Hauser, J. A. King, R. M. Pagel and J. M. Keith, *J. Appl. Polym. Sci.*, 2008, **109**, 2145–2155.

143 T. Ji, Y. Feng, M. Qin, S. Li, F. Zhang, F. Lv and W. Feng, *Carbon*, 2018, **131**, 149–159.
144 I. M. Afanasov, D. V. Savchenko, S. G. Ionov, D. A. Rusakov, A. N. Seleznev and V. V. Avdeev, *Inorg. Mater.*, 2009, **45**, 486–490.
145 H. Li, S. Wu, J. Wu and G. Huang, *Colloid Polym. Sci.*, 2013, **291**, 2279–2287.
146 J. Han, X. Yang, L. Liao, G. Zhou, G. Wang, C. Xu, W. Hu, M. E. R. Debora and Q. Song, *Nano Energy*, 2019, **58**, 331–337.
147 A. Chizhov, M. Rumyantseva and A. Gaskov, *Nanomaterials*, 2021, **11**, 892.
148 P. Cui, D. Wei, J. Ji, H. Huang, E. Jia, S. Dou, T. Wang, W. Wang and M. Li, *Nat. Energy*, 2019, **4**, 150–159.
149 X. L. Shi, K. Zheng, W. D. Liu, Y. Wang, Y. Z. Yang, Z. G. Chen and J. Zou, *Adv. Energy Mater.*, 2018, **8**, 1800775.
150 P. P. Altermatt, A. Schenk, F. Geelhaar and G. Heiser, *J. Appl. Phys.*, 2003, **93**, 1598–1604.
151 C. Cao, H. Dong, F. Liang, Y. Zhang, W. Zhang, H. Wang, H. Shao, H. Liu, K. Dong, Y. Tang, Y. Lai and M. Ge, *Chem. Eng. J.*, 2021, **416**, 129094.
152 M. Ge, Y. Tang, O. I. Malyi, Y. Zhang, Z. Zhu, Z. Lv, X. Ge, H. Xia, J. Huang, Y. Lai and X. Chen, *Small*, 2020, **16**, 2002094.
153 X. Chen, T. Jiang, Y. Yao, L. Xu, Z. Zhao and Z. L. Wang, *Adv. Funct. Mater.*, 2016, **26**, 4906–4913.
154 Y. Yang, H. Zhang, J. Chen, Q. Jing, Y. S. Zhou, X. Wen and Z. L. Wang, *ACS Nano*, 2013, **7**, 7342–7351.
155 S. S. K. Mallineni, Y. Dong, H. Behlow, A. M. Rao and R. Podila, *Adv. Energy Mater.*, 2018, **8**, 1702736.
156 A. Li, Y. Zi, H. Guo, Z. L. Wang and F. M. Fernández, *Nat. Nanotechnol.*, 2017, **12**, 481–487.
157 T. Namaguchi and H. Uchida, *Electrical Overstress/Electrostatic Discharge Symposium Proceedings 1998 (Cat. No. 98TH8347)*, IEEE, 1998, pp. 245–251.
158 K. L. Yam, *The Wiley Encyclopedia of Packaging Technology*, John Wiley & Sons, 2010.
159 H. Lei, Y. Chen, Z. Gao, Z. Wen and X. Sun, *J. Mater. Chem. A*, 2021, **9**, 20100–20130.
160 S. Hasegawa and F. Grey, *Surf. Sci.*, 2002, **500**, 84–104.
161 D. K. Das-Gupta, *IEEE Trans. Electr. Insul.*, 1992, **27**, 909–923.
162 B. Zhang and G. Zhang, *J. Appl. Phys.*, 2017, **121**, 105105.
163 S. Al-Malaika, F. Axtell, R. Rothon and M. Gilbert, in *Brydson's Plastics Materials*, Elsevier, 2017, pp. 127–168.
164 G. Wypych and J. Pionteck, *Handbook of Antistatics*, Elsevier, 2016.
165 H. T. M. Haenen, *J. Electrost.*, 1975, **1**, 173–185.
166 T. A. L. Burgo, C. A. Rezende, S. Bertazzo, A. Galembeck and F. Galembeck, *J. Electrost.*, 2011, **69**, 401–409.
167 R. E. Hirschberg, M. Scharnberg, S. Schröder, S. Rehders, T. Strunskus and F. Faupel, *Org. Electron.*, 2018, **57**, 146–150.
168 T. A. L. Burgo, L. B. S. Balestrin and F. Galembeck, *Polym. Degrad. Stab.*, 2014, **104**, 11–17.
169 R. M. Pashley, M. Rzechowicz, L. R. Pashley and M. J. Francis, *J. Phys. Chem. B*, 2005, **109**, 1231–1238.
170 J. A. Wiles, M. Fialkowski, M. R. Radowski, G. M. Whitesides and B. A. Grzybowski, *J. Phys. Chem. B*, 2004, **108**, 20296–20302.
171 Y. Awakuni and J. H. Calderwood, *J. Phys. D: Appl. Phys.*, 1972, **5**, 1038.
172 G. Dubey, G. P. Lopinski and F. Rosei, *Appl. Phys. Lett.*, 2007, **91**, 232111.
173 V. T. C. Paiva, L. P. Santos, D. S. da Silva, T. A. L. Burgo and F. Galembeck, *Langmuir*, 2019, **35**, 7703–7712.
174 J. D. Jeyaprakash, S. Samuel, P. Ruther, H.-P. Frerichs, M. Lehmann, O. Paul and J. Rühe, *Sens. Actuators, B*, 2005, **110**, 218–224.
175 M. T. Byrne and Y. K. Gun'ko, *Adv. Mater.*, 2010, **22**, 1672–1688.
176 H. Wang, G. Xie, M. Fang, Z. Ying, Y. Tong and Y. Zeng, *Composites, Part B*, 2015, **79**, 444–450.
177 R. M. Scarisbrick, *J. Phys. D: Appl. Phys.*, 1973, **6**, 2098.
178 M. Layani, M. Gruchko, O. Milo, I. Balberg, D. Azulay and S. Magdassi, *ACS Nano*, 2009, **3**, 3537–3542.
179 A. Mirmohseni, M. Azizi and M. S. S. Dorraji, *Prog. Org. Coat.*, 2019, **131**, 322–332.
180 Y.-J. Park, S. Y. Park and I. In, *J. Ind. Eng. Chem.*, 2011, **17**, 298–303.
181 J.-Y. Xue, J.-H. Chen, J.-H. Dong, H. Wang, W.-D. Li, J.-B. Deng and G.-J. Zhang, *J. Phys. D: Appl. Phys.*, 2019, **52**, 405502.
182 G. Wulff, L. Zhu and H. Schmidt, *Macromolecules*, 1997, **30**, 4533–4539.
183 E. T. Kang, K. G. Neoh, K. L. Tan, B. C. Senn, P. J. Pigram and J. Liesegang, *Polym. Adv. Technol.*, 1997, **8**, 683–692.
184 Y. Kugimoto, A. Wakabayashi, T. Dobashi, O. Ohnishi, T. K. Doi and S. Kurokawa, *Prog. Org. Coat.*, 2016, **92**, 80–84.
185 K. B. Lim, B. S. Lee, J. T. Kim and D. C. Lee, *Surf. Interface Anal.*, 2002, **33**, 918–923.
186 J. A. Vickers, M. M. Caulum and C. S. Henry, *Anal. Chem.*, 2006, **78**, 7446–7452.
187 T. Shao, F. Liu, B. Hai, Y. Ma, R. Wang and C. Ren, *IEEE Trans. Dielectr. Electr. Insul.*, 2017, **24**, 1557–1565.
188 A. Crisci, B. Gosse, J. P. Gosse and V. Ollier-Duréault, *Eur. Phys. J.: Appl. Phys.*, 1998, **4**, 107–116.
189 Textile Exchange, *Preferred Fiber & Materials Market Report 2021*, 2021.
190 G. Liu, Z. Wang, B. Bao, Z. Ouyang, C. Du, F. Liu, W. Wang and D. Yu, *J. Colloid Interface Sci.*, 2021, **588**, 50–61.
191 Z. Zhang, Y. Cao, J. Gu, J. Li, Y. Wang and S. Chen, *Mater. Today Chem.*, 2021, **22**, 100571.
192 J. Zhang, C. Su, F. J. M. Rogers, N. Darwish, M. L. Coote and S. Ciampi, *Phys. Chem. Chem. Phys.*, 2020, **22**, 11671–11677.
193 R. Valdivia-Barrientos, J. Pacheco-Sotelo, M. Pacheco-Pacheco, J. S. Benítez-Read and R. López-Callejas, *Plasma Sources Sci. Technol.*, 2006, **15**, 237.
194 J. Seo, S. Hajra, M. Sahu and H. J. Kim, *Mater. Lett.*, 2021, **304**, 130674.
195 C. B. Duke, J. Noolandi and T. Thieret, *Surf. Sci.*, 2002, **500**, 1005–1023.
196 S. Bendimerad, A. Tilmatine, M. Ziane and L. Dascalescu, *Int. J. Environ. Stud.*, 2009, **66**, 529–538.

197 B. A. Grzybowski, A. Winkleman, J. A. Wiles, Y. Brumer and G. M. Whitesides, *Nat. Mater.*, 2003, **2**, 241–245.
198 Y. Bai, C. B. Han, C. He, G. Q. Gu, J. H. Nie, J. J. Shao, T. X. Xiao, C. R. Deng and Z. L. Wang, *Adv. Funct. Mater.*, 2018, **28**, 1706680.
199 S. Chen, T. Huang, H. Zuo, S. Qian, Y. Guo, L. Sun, D. Lei, Q. Wu, B. Zhu, C. He, X. Mo, E. Jeffries, H. Yu and Z. You, *Adv. Funct. Mater.*, 2018, **28**, 1805108.
200 H. Yang, Y. Pang, T. Bu, W. Liu, J. Luo, D. Jiang, C. Zhang and Z. L. Wang, *Nat. Commun.*, 2019, **10**, 1–7.
201 Z. Wang, J. An, J. Nie, J. Luo, J. Shao, T. Jiang, B. Chen, W. Tang and Z. L. Wang, *Adv. Mater.*, 2020, **32**, 2001466.
202 S. Niu, X. Wang, F. Yi, Y. S. Zhou and Z. L. Wang, *Nat. Commun.*, 2015, **6**, 1–8.
203 Q. Zheng, B. Shi, F. Fan, X. Wang, L. Yan, W. Yuan, S. Wang, H. Liu, Z. Li and Z. L. Wang, *Adv. Mater.*, 2014, **26**, 5851–5856.
204 Y. Liu, S. Niu and Z. L. Wang, *Adv. Electron. Mater.*, 2015, **1**, 1500124.
205 B. Kaczer, R. Degraeve, P. Roussel and G. Groeseneken, *Microelectron. Reliab.*, 2007, **47**, 559–566.
206 Z. W. Yang, Y. Pang, L. Zhang, C. Lu, J. Chen, T. Zhou, C. Zhang and Z. L. Wang, *ACS Nano*, 2016, **10**, 10912–10920.
207 L. C. Kloth, *Adv. Wound Care*, 2014, **3**, 81–90.
208 W. Hu, X. Wei, L. Zhu, D. Yin, A. Wei, X. Bi, T. Liu, G. Zhou, Y. Qiang, X. Sun, Z. Wen and Y. Pan, *Nano Energy*, 2019, **57**, 600–607.
209 M. Le Bras, M. V. Clement, S. Pervaiz and C. Brenner, *Histol. Histopathol.*, 2005, **20**, 205–220.
210 Q. Zhang, Q. Liang, Q. Liao, M. Ma, F. Gao, X. Zhao, Y. Song, L. Song, X. Xun and Y. Zhang, *Adv. Funct. Mater.*, 2018, **28**, 1803117.
211 H. Yuan, H. Yu, X. Liu, H. Zhao, Y. Zhang, Z. Xi, Q. Zhang, L. Liu, Y. Lin, X. Pan and M. Xu, *Nanomaterials*, 2021, **11**, 3431.
212 Y. Feng, L. Ling, J. Nie, K. Han, X. Chen, Z. Bian, H. Li and Z. L. Wang, *ACS Nano*, 2017, **11**, 12411–12418.
213 J. Yang, H. Wang, G. Zhang, X. Bai, X. Zhao and Y. He, *Resour., Conserv. Recycl.*, 2019, **146**, 264–269.
214 H. Lei, M. Wu, F. Mo, S. Ji, X. Dong, Z. Wu, J. Gao, Y. Yang and Y. Jia, *Nano Energy*, 2020, **78**, 105290.
215 C. Park, G. Song, S. M. Cho, J. Chung, Y. Lee, E. H. Kim, M. Kim, S. Lee, J. Huh and C. Park, *Adv. Funct. Mater.*, 2017, **27**, 1701367.
216 Q. Shi, H. Wang, H. Wu and C. Lee, *Nano Energy*, 2017, **40**, 203–213.